Directed Biogenic Fabrication: Programming Cells and Their Ecosystems to Grow Civil Infrastructure

Joshua Van Zak

Bachelor of Arts in Urban Planning and Visual Arts,
University of California, San Diego, 2011

Submitted to the Program in Media Arts and Sciences,
School of Architecture and Planning,
in partial fulfillment of the requirements for the degree of
Master of Science in Media Arts and Sciences at the

MASSACHUSETTS INSTITUTE OF TECHNOLOGY

June, 2019

Signature redacted

Author, Joshua Van Zak
Program in Media Arts and Sciences
May 20, 2018

Signature redacted

Certified by Neri Oxman
Associate Professor of Media Arts and Sciences
Thesis Advisor

Signature redacted

Accepted by Tod Machover
Academic Head
Program in Media Arts and Sciences

Directed Biogenic Fabrication: Programming Cells and Their Ecosystems to Grow Civil Infrastructure

Joshua Van Zak

Submitted to the Program in Media Arts and Sciences,
School of Architecture and Planning,
in partial fulfillment of the requirements for the degree of
Master of Science in Media Arts and Sciences

Abstract

This thesis introduces and evaluates *directed biogenic fabrication*: a philosophical approach and technical framework for co-fabricating ecologically active civil infrastructure with living cells. I propose that imbuing our buildings and urban systems with life, or at least biologic capabilities, will enable tight interconnections between fundamental species occupying different infrastructural niches, resulting in urban ecosystems that develop and evolve closed-loop resource cycles and equilibrate our atmosphere. As a proof of concept for this generalizable approach, I cover three strategies demonstrating specific tools, techniques, and assessment methods for designing elements of a living infrastructure: (1) *Programmable Surface Features and Hydrophilicity*—utilizing organic chemistry, computational design, and digital fabrication to engender particular mechanical properties and responsiveness in biopolymer materials; *Communication Ecology*—templating visual and conformational signals in biopolymer materials that communicate information about the environment to other organisms; and *Opportunistic Chimeric Design*—exploiting and co-opting the most powerful capabilities evolution has produced in order to grow infrastructural lifeforms. The first two methods are exemplified through two architectural scale pavilions—Aguahoja I and II—while the third is shown through a series of prototypical materials synthesized by two types of bone cancer cells. This thesis makes contributions to the fields of materials science, biological engineering, civil engineering, digital fabrication, and computational design.

Thesis Supervisor: Neri Oxman
Title: Associate Professor of Media Arts and Sciences, Program in Media Arts and Sciences

Directed Biogenic Fabrication:
Programming Cells and Their Ecosystems to Grow Civil Infrastructure

Joshua Van Zak

Submitted to the Program in Media Arts and Sciences,
School of Architecture and Planning,
in partial fulfillment of the requirements for the degree of
Master of Science in Media Arts and Sciences

Signature redacted

Thesis Reader, *Dr. Robert Langer*,
David H. Koch Institute Professor,
Koch Institute for Integrative Cancer Research at MIT

Directed Biogenic Fabrication: Programming Cells and Their Ecosystems to Grow Civil Infrastructure

Joshua Van Zak

Submitted to the Program in Media Arts and Sciences,
School of Architecture and Planning,
in partial fulfillment of the requirements for the degree of
Master of Science in Media Arts and Sciences

Signature redacted

Thesis Reader, *Dr. Pamela Silver,*
Elliot T. and Onie H. Adams Professor of Biochemistry and Systems Biology,
Harvard Medical School

Acknowledgements

At the end of our lives, we'll have had a quantifiable number of happy moments. Everyone I thank below has contributed to a favorable margin in this proportion, and I will be forever grateful to each of you. As I move onto the next stage of my life, I hope to do the same for others.

First and foremost, my parents have raised me to be curious and driven, and to embrace my uniqueness. These qualities and the sacrifices you've made have enabled me to get to where I am today. This small paragraph is not nearly enough to adequately thank you.

To the rest of my family, your constant support, humor, and togetherness in the face of adversity have inspired and amazed me. To Laura, your humor, support, and love have made life fun and exciting; I can't imagine a better gift. Thank you.

To Neri, others admire you because of the beautiful things you create, but it's your ability to bring beauty out of the most obscure and special places that I find most inspirational. My life and those of my family members have dramatically changed because it. For this reason, I also want to thank Jorge Duro-Royo, Natalia Casas, Priscilla Capistrano, and Kelly Egorova for their generosity and sustained belief in me.

To the rest of the Mediated Matter family as well as my thesis readers, professors—especially, Chris Fry, Pam Silver, Tim Lu, and Hiroshi Ishii—and friends, I hope to apply what you have taught me to most effectively utilize my time on this planet to make it better.

Finally, I would like to thank GETTYLAB, the MIT-Sensetime Project, the MIT Skoltech Program, and the MIT Sandbox Innovation Fund for their financial support. I would also like to thank the Cooper-Hewitt Smithsonian Design Museum, San Francisco Museum of Modern Art, Centre Pompidou, and Cube Design Museum for showing our projects.

Contents

Figures

Introduction

Ironically, the structures and products we put thought and effort into building are never as sophisticated as our own bodies. Both are just aggregates of matter and energy, but the difference in planetary value between the things we design and the functionality inside us results from billions of years of evolution. This would be a minor problem if we were simply underutilizing evolutionary intelligence; however, driving infrastructural development with anthropocentric utility has obscured the fact that we should occupy an ecological niche.

In un-humanized ecosystems, the most fruitful shelter comes in the form of other living things. Specifically, omnidirectional forces drive biologic design. Since there are finite stores of matter and energy, ideal equilibria exist between the number and size of organisms, how long they live, how they impact the energy flows and living things around them, and how they return to the resource cycles they came from.

Primary producers such as plants get energy from the sun and simple organic matter. Consumers ingest plants and other consumers. Decomposers such as bacteria, molds, and fungi make use of energy stored in dead plant and animal tissues. In this process, matter and energy are moved through resource cycles that equilibrate the atmospheric and ecological conditions on earth.

An organism's ability to do so relies on constant dynamism between a changing environment, genetic and behavioral adaptation, and strategic symbioses between and within ecological niches. The movement of matter and energy through this process creates a resource cycle that entraps, transforms, and replenishes resource inventories, with minimal losses. Accordingly, primal desires to consume sufficient calories and shelter oneself from environmental extrema drive a set of behaviors and physical adaptations that, without conscious effort, enables interdependent ecological niches to construct and maintain an entire ecosystem.

Therefore, the design of living things must take into consideration factors pertaining to immediate functional requirements such as basic physiologic needs, competition for resources, and environmental conditions, as well as factors relating to their role within a larger ecosystem.[1] This is the difference between a tree and a log cabin. Toward this end, humans have developed an ability to conceptualize, organize, and design complex systems such as urban infrastructure and the genome itself. We now need to utilize these abilities to design ecosystems that more purposefully and precisely codify infrastructural niches in order to equilibrate our atmosphere.

In organisms, physiologic mechanisms guiding the entrapment, transformation, and replenishment of energy dictate the more conserved features of biologic development such as axial symmetry and skeletal structure, while those that have to do with fitness iterate through more malleable prototypes. Functionally, complex combinations of molecules assemble into cells, cells construct tissues, tissues form organs, organs coordinate to create organ systems, and multiple systems interact to perform complex functions. Some examples include thermoregulation, reproduction, self-healing, coordinated thought processes and actuation, derivation of energy from its surrounding resources, and learning/optimizing behavior and physiology over time. The result is a dynamic structure that grows from, consumes, transforms, and restores the matter and energy that comprise its habitat. Imagine if our buildings could do this.

Conversely, in manmade materials, great care is taken to ensure that uniformity, unifunctionality, durability, and stasis are given preference over the aforementioned dynamism. In fact, the inputs that are processed to become 'synthetic' materials come from the world around us; whereas, it is their recombination, processing, and behavior that make them detrimental to our planet. In rebranding 'synthetic' materials as 'manmade,' we can apply a common set of metrics to every piece of matter around us that pertains to both their immediate utility and reliability as well as their ecosystemic value.

As a simple example, a typical architect will design spaces based on the events that are supposed to occur in them. The organization of these spaces would be configured to facilitate sequences of events that make sense together and/or make life easier. Finally, the shape and material of the building would ideally be chosen based on the context around it. Conversely, an architectural symbiont that occupies part of an ecological niche would grow from its habitat, derive energy from the resources around it, convert food into energy, and secrete waste products that feed other consumers.

If over 7 billion large, long-lived organisms consume massive amounts of resources for their own growth and to support densely packed communities, then severe bottlenecks develop in resource continua. Industrial innovations such as paving over entire biomes, extracting massive amounts of resources and transforming them into materials that degrade over hundreds-to-thousands of years, and developing manufacturing processes that saturate the atmosphere with harmful gases and consume great amounts of energy drive out other producers, consumers, and degraders. Just think about how many things are not human or human-made on the route to work.

In the absence of such a dominating species, ecosystems equilibrate almost haphazardly, with each ecological niche being filled by organisms acting in their best interest. This is why, given our ability to conceptualize and organize complex systems at a massive scale, humans are equipped to direct the biogenesis of ecofunctional infrastructure. Importantly, giving preference to materials that are recyclable and infrastructure that requires less energy input is not the same as designing ecosystems that perpetually and autonomously recycle matter and energy.

More generally, there are two approaches to solving large problems: one is to reduce issues to their contributing factors, after which an immediate solution is created for each; alternatively, entire systems can be redesigned based on evolved intelligence. Although I have come far

short of doing the latter in this thesis, I think it is valuable to define a potentially transformative theoretical framework and execute early experiments toward it.

In **Part 1** of the thesis, I describe chemical and fabrication methods of programming specific mechanical properties and behaviors into biopolymer materials for buildings and products. These are exemplified through several experiments and analyses that culminated in a five-meter tall, biopolymer-based pavilion, Aguahoja I, that was designed to dissociate in water. **Part 2** builds on this ecofunctional design with visual and conformational signals in biopolymer materials that communicate information about the environment to other organisms, as shown in a second pavilion, Aguahoja II. Subsequently, **Part 3** introduces *opportunistic chimeric design*, which involves co-opting the most powerful capabilities evolution has produced in order to grow multifunctional structures and products. The conclusion of Part 3 presents the implications and potential future directions of this research, with the hope of inspiring others to rethink how we solve global problems.

Part 1 — Aguahoja I

1.1 Rationale

The Aguahoja Pavilion is a five-meter tall prototype demonstrating that buildings can be synthesized from organic waste streams and dissociated in water, or biodegraded, to return to the resource cycles they came from. We utilized our planet's most abundant biopolymers including chitosan from shrimp shells, pectin from apple skins, and cellulose from dead plant matter to create tunable hydrogels that were pneumatically extruded using a robotic arm.

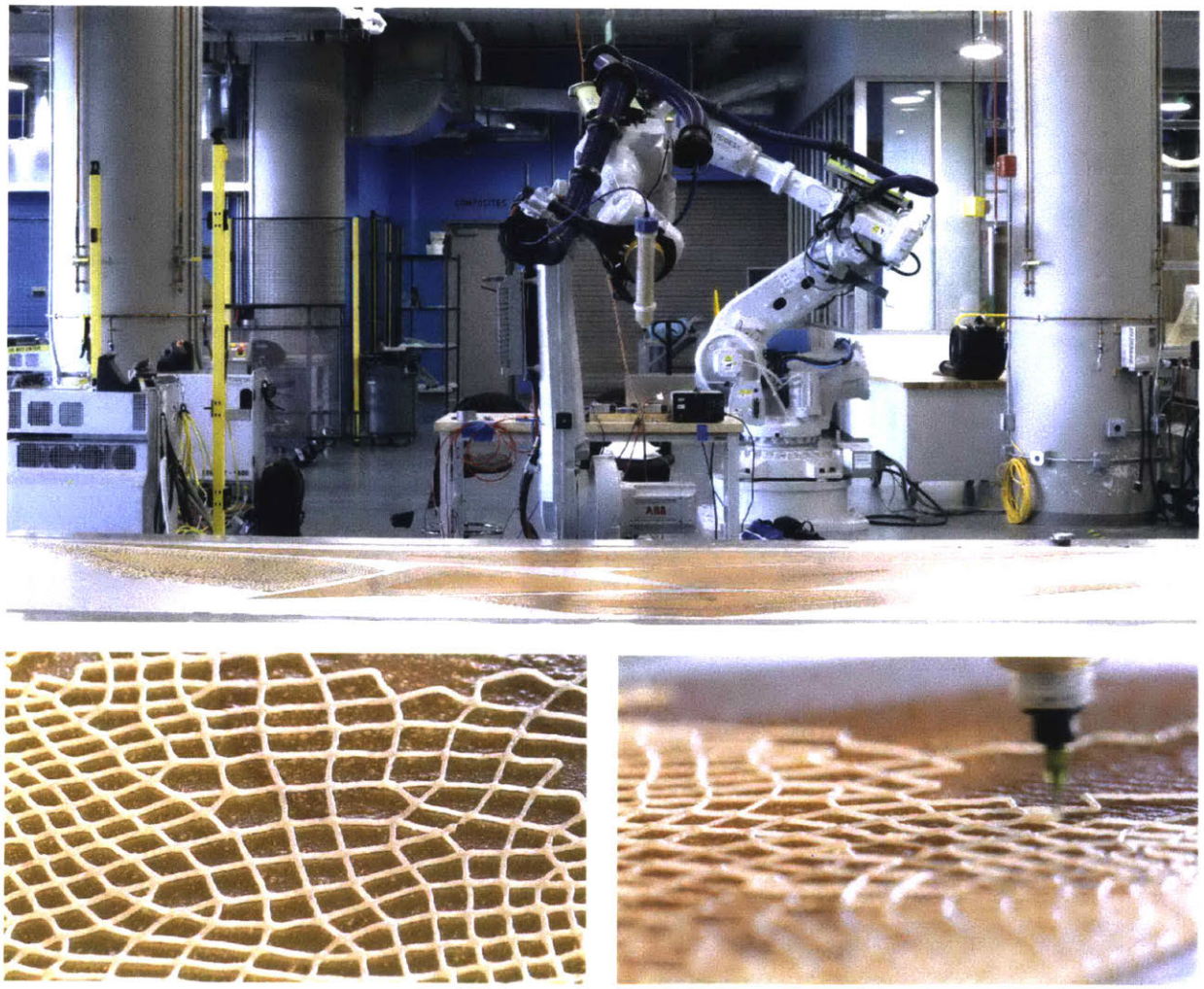

Figure 1.1 — Fabrication images of a 6-axis ABB 4600 robotic arm and custom pneumatic extrusion end-effector.[2]

Figure 1.2 — The Aguahoja Pavilion at the MIT Media Lab, spring, 2018.
Photo credit: Yen-Ju Tai.

1.2 Anatomy

Aguahoja I consists of 32 composite panels slotted into a five-meter tall, 3D printed structure. Depending on the ambient temperature and relative humidity, the panels oscillate between exhibiting significant plasticity, like a leather, and rigidity, like balsa wood. Such climatic changes also induce conformational adaptation that manifests as curling, when water is evaporated, and relaxing, when water is absorbed. To achieve this behavior, flexible pectin-chitosan skins are functionalized in key locations by rigid chitosan-cellulose shell patterns.

Skin: Apple pectin (Spectrum Chemicals & Laboratory Products, New Brunswick, NJ) was chosen as a skin material because of its opposite charge to chitosan as well as its tunability. Specifically, pectin's galacturonic acid units have negatively charged carboxylic groups that enable it to form a polyelectrolyte complex with polycationic chitosan.[3] Chitosan (85% de-acetylated, molecular weight = 100,000, VWR, Radnor, PA) is soluble in acidic, alkaline, and neutral solvents, while pectin is highly water-soluble. Thus, pectin could be used as a crosslinker to form a polyelectrolyte complex.

A polyelectrolyte (PE) is any macromolecular material that has repeating units and dissociates into a highly charged polymer in an ionizing solvent like water.[4] These repeating ionized units can be neutralized by smaller, oppositely charged counter ions that maintain a net neutral charge. While in this uncharged state, PEs behave like other macromolecules; however, significant changes in their bulk properties can result from small dissociations of ionic groups.[5]

Partial or complete dissociation of ionic groups can cause electrostatic interactions that dramatically alter a polymer's behavior. If new ionic groups are introduced, hydrogel properties such as viscosity, solubility, pH, ionization constant, ionic strength, and diffusion coefficient can be altered.[6] In particular, the ionic strength of a solution influences its properties and those of the resulting film. Low ionic strength causes PEs to extend because of intramolecular repulsive forces. Increasing the ionic strength of a PE solution tends to make it thicker.[7]

Many properties of interest can be controlled in such interpolymer complexes, which, after hydrogels are printed and dried at room temperature, imbue the resulting skins with tunable mechanical and optical properties.[8] Some knobs one can turn in PE chemistry are the degree of ionization and charge distribution on PEs; ionic group attributes; strength of ionic sites; pH; molecular weight; polymer structure; degree of complexation; density; concentration; chain stiffness; mixing ratio, order, duration, and technique; temperature conditions while mixing, printing, and drying; and hydrophilicity.[9,10]

This *parametric chemistry*[2] enabled us to tune the properties of both the hydrogel and the resulting film according to desired fabrication and performance parameters. With respect to fabrication, a custom pneumatic end-effector was created for a six-axis ABB 4600 robotic arm (ABB Robotics, Zurich, Switzerland) to extrude multiple hydrogels.[11] Thus, the viscosity of the hydrogels was the first parameter that needed to be tuned with respect to the capacity of the air compressor and desired spread function—i.e., how much the gel would spread out on the print bed in relation to the nozzle diameter. The spread function, S, is defined as follows:

$$S = \frac{Printed\ line\ diameter - Nozzle\ diameter}{Nozzle\ diameter}$$

Accordingly, an ideal baseline concentration of pectin was determined to be 35% (w/v) in water, because the spread function (S = 0.26) enabled us to fill in the outline of a panel with parallel lines for the printer to follow that were 2 mm apart, using a 1.58 mm nozzle, such that the lines would bleed into each other and create a thin film. The spread function decreased linearly with viscosity—i.e., the concentration of pectin—up to a maximum pectin concentration of 45% (w/v), or 1,200 centipoise at room temperature, requiring 60 p.s.i. of air pressure. Herein, factorial combinations of nozzle diameter, height from the table, robotic feed rate, and air pressure could be iterated through to find optimal combinations of material properties and fabrication parameters for particular designs.

Next, the mechanical and optical properties of the pectin skins had to be considered. By adding up to 8% (w/v) of chitosan into an acidic or alkaline solution, pectin skins could be rigidified, thickened, and colored via the creation of polyelectrolyte complexes. With the addition of up to 5% (v/v) of glycerin, the plasticity and ductility of the films could be finely tuned. At pectin concentrations over 40% (w/v) and chitosan concentrations over 2% (w/v), shape memory could be developed in the films by printing them over or steaming them onto various molds.

The formation of pectin-chitosan polyelectrolyte complexes was confirmed via differential scanning calorimetry (DSC) (DSC 250, TA Instruments, New Castle, DE). It should be noted that DSC alone is insufficient to properly confirm the existence and properties of a polyelectrolyte complex, and that only one pectin-chitosan combination (35% apple pectin (w/v), 2% chitosan (w/v), 1% glacial acetic acid (v/v), 2% vegetable glycering (v/v)) was tested.

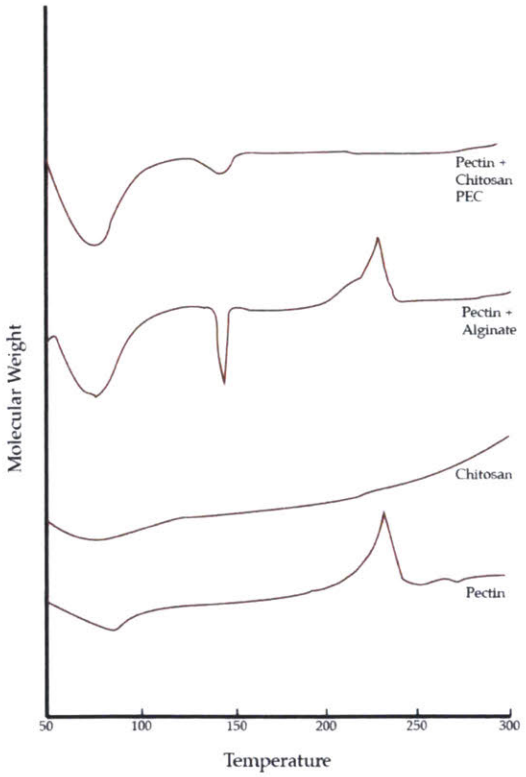

Figure 1.3 — Differential scanning calorimetry of hydrogels containing 35% apple pectin (w/v) in water, 2% chitosan (w/v) in water, 35% apple pectin (w/v) and 2% alginate (w/v) in water, and 35% apple pectin (w/v) and 2% chitosan (w/v) in water, to confirm the formation of a polyelectrolyte complex between pectin and chitosan.

Moreover, the toolpath geometry that the robotic arm would follow when printing the skins would engender isotropy or anisotropy, depending on its symmetry. Although this phenomenon was not sufficiently studied during this project, it is of interest for future research.

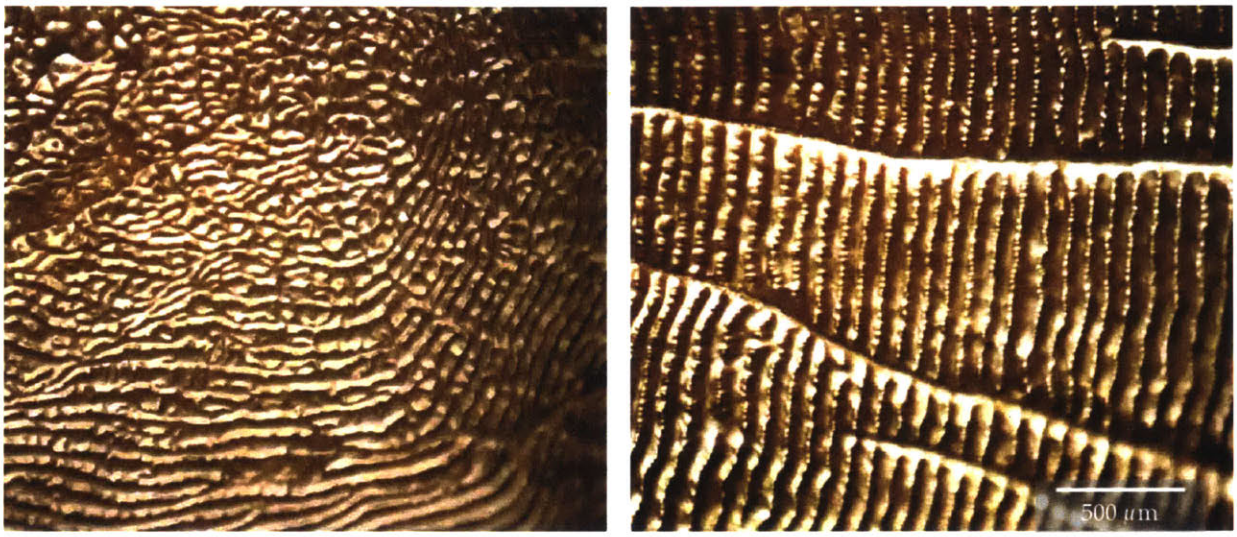

Figure 1.4 — Pectin's isotropic dependence on toolpath geometry.

Shell: Despite the aforementioned tunable parameters, printing pectin or pectin-chitosan hydrogels into shapes that were 1-2 meters long resulted in skins that lacked mechanical integrity and significant responsiveness. Thus, chitosan-cellulose composites and geometric patterns were designed to rigidify the skins in key locations and along specific axes, like a shell.

Specifically, a structural layer consisting of 7% chitosan (w/v), 3.5% glacial acetic acid (v/v), 45% cellulose pulp (v/v), and 0.7% glycerin (v/v) was printed onto pectin skins that varied in composition across one panel. Water was heated to 78°C, at which point chitosan powder was stirred in. The solution temperature was then lowered to 37°C, and acetic acid was mixed in with a hand mixer. After the solution gelled, cellulose pulp was slowly sifted in to form a viscous hydrogel, which was then homogenized with a hand mixer.[2]

Here, we took advantage of the fact that chitosan and cellulose polymers physically interweave and thereby rigidify each printed line as they dried at room temperature. Toolpaths based on a distorted grid or regular lattice could then be generated to create a shrinking mesh network that would embed tension into the panels as the pectin countervailed these contractile forces.

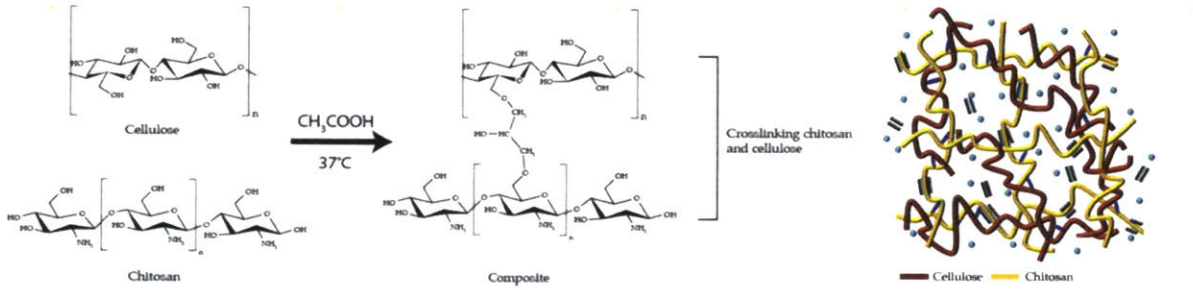

Figure 1.5 — Physical crosslinking of chitosan and cellulose (adapted from Tu *et al.*, 2017).[12]

Fabrication: Following mixing, 300 ml of the chitosan-cellulose hydrogel were loaded into a 360 ml plastic cartridge (Nordson Corporation, Westlake, OH). Resolution was an important design parameter in this case, so the spread function had to be minimized (<0.05) and viscosity tuned (>200 centipoise) to enable a nozzle with a diameter of 0.79 mm to be used to print lines that were less than 0.9 mm in diameter.

After loading a piston into a cartridge to push down the material, the cartridge was loaded into a holster on our pneumatic end-effector. Finally, a cap was screwed on and connected via tubing to an air compressor.

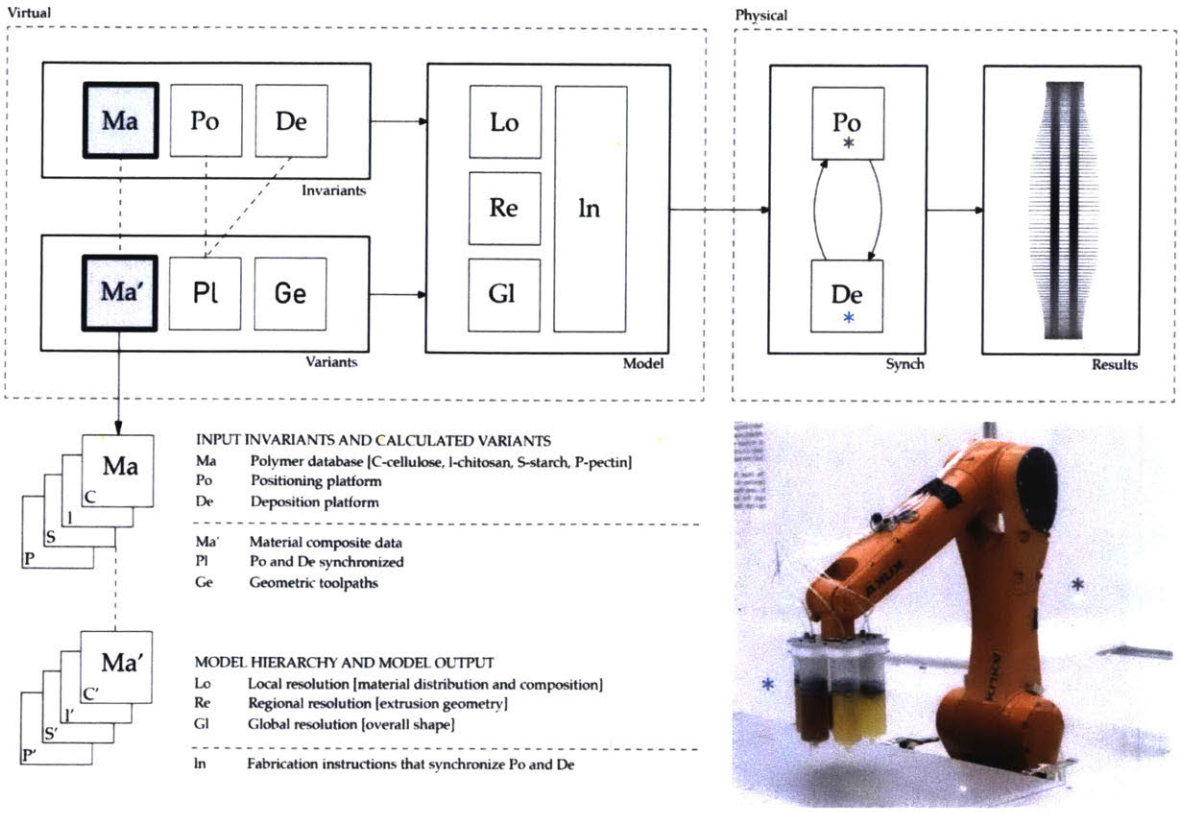

Figure 1.6 — Interdependence of material properties, computational inputs, and fabrication parameters.[2]

Input geometry and fabrication parameters were defined in Rhinoceros 3D and Grasshopper, from which a G-code file was generated. This file fed coordinate points to the robotic arm and specified air pressure, speed, and height from the substrate. The arm was initially calibrated using the four corner points and center point of a 1.5 m x 3 m print table.

1.3 Physiology

After printing the chitosan-cellulose shell pattern onto dry pectin-chitosan skins, losing water and drying at room temperature at different rates, in different spots, would cause the shell material to shrink bidirectionally and warp about the major axis of each panel, in the case of longitudinal lines, and about the minor axis of each panel in the case of latitudinal lines. In turn, the pectin skin could be specifically designed to not only countervail these deformations, but also utilize this energy to rigidify a panel.

Given that pectin has an opposite charge to chitosan, the two polymers electrostatically attracted each other when wet chitosan and cellulose was printed onto dry pectin-chitosan skins. This helped countervail the contractile forces of a chitosan-cellulose hydrogel that was ~80% water and would lose much of its mass and volume due to evaporation. In addition, creating toolpaths based on a distorted grid or regular lattice helped deflect these forces through interpenetrating kinked and curved mesh networks.[13]

In a regular lattice, contractile forces were locally concentrated at the midpoints of each set of interpenetrating lines, almost like two connected rubber rods were being pulled away from each other. Globally, this would create bowing emanating bidirectionally from the centroid of each panel. This resulted in a shell-like conformation, with stresses being concentrated at the top of the shell. By selectively printing additional chitosan-cellulose layers on top of certain lines traveling along major or minor axes, the conformation and stress concentration could be tuned, in order to imbue a panel with the desired mechanical behavior.

Conversely, a distorted grid, assuming uniform line diameter and layer quantity, could locally deflect contractile forces to imbue a panel with functionally graded behavior, based on the convergence and divergence of lines. Further modifying the number of layers along certain paths, composition of the shell material, fabrication parameters, as well as the mixing and drying conditions enabled us to finely tune the mechanical properties of skin-shell composites for particular use cases.

Importantly, absorption of humidity and rain, in addition to temperature fluctuations, would cause contraction or relaxation, which could elicit specific conformational changes in each panel, depending on the printed geometry. In the future, these behaviors could provide thermoregulation and responsive shading in buildings.

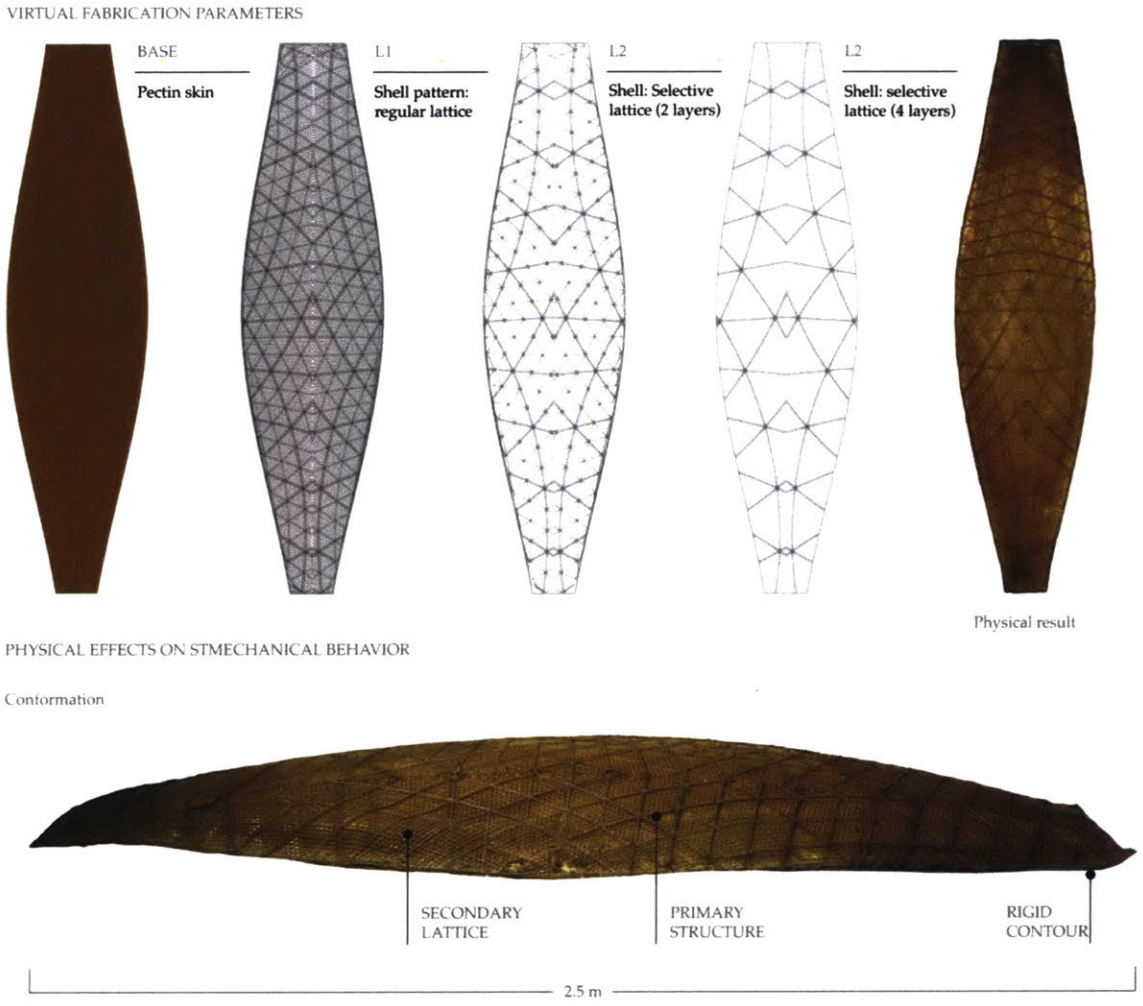

Figure 1.7 — Skin-shell interplay in relation to toolpath geometry, based on a selectively reinforced lattice.[2]

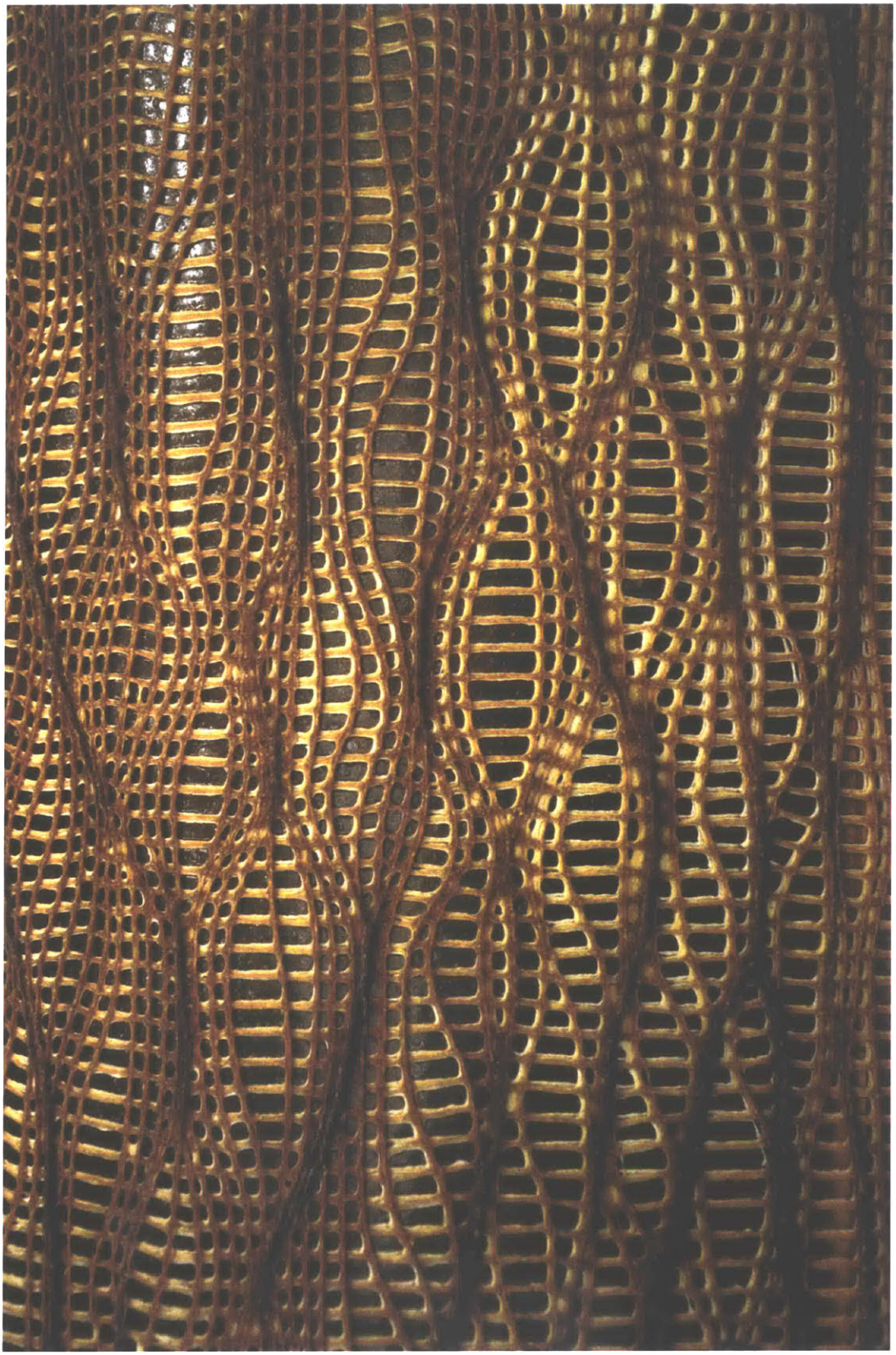

Figure 1.8 — Closeup of the chitosan-cellulose shell composite on pectin skin (35% pectin (w/v), 3% glycerin (v/v) in water), following a distorted grid toolpath. Photo: Yen-Ju Tai.

Tunable Surface Features and Hydrophilicity: Based on such resistance to contractile forces, significant dynamism could be designed into the fabrication process by introducing new ionic groups and fillers into the pectin skins. Surface roughness, hydrophilicity, water adsorption, and hysteresis could be finely tuned in the dried skin.[14] Regarding fabrication parameters, low ionic strength in the hydrogel enabled shear thinning during the printing process; whereas, increasing the ionic strength made the solution thicker in almost all cases. Printing denser materials often increased their tensile strength and elasticity, so modulating density independently of viscosity was an important research path to pursue.

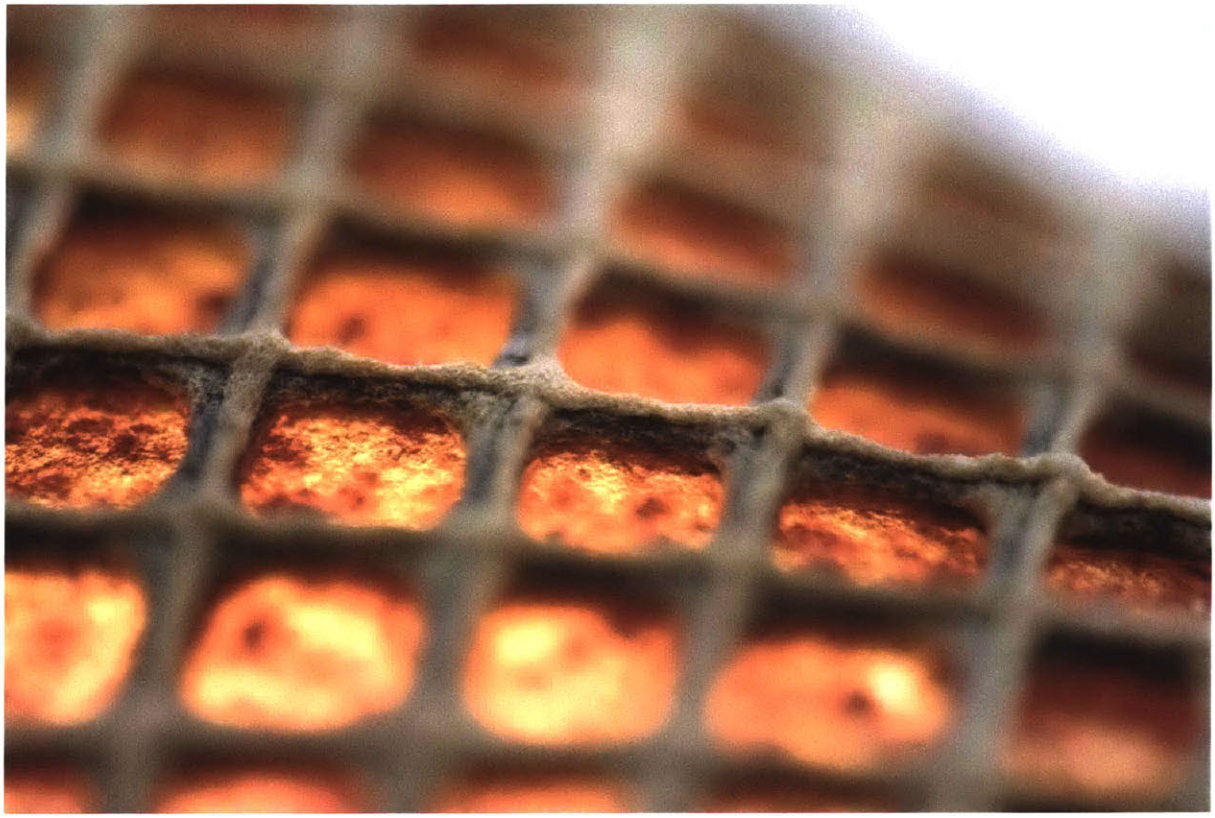

Figure 1.9 — Demonstration of how water absorption in the pectin skin influenced the color and mechanical properties of the chitosan-cellulose shell material. The darker color in the bottom layer of shell lines indicated that water had been absorbed by the skin below, resulting in a darker, more rigid material. Photo: Joao Costa.

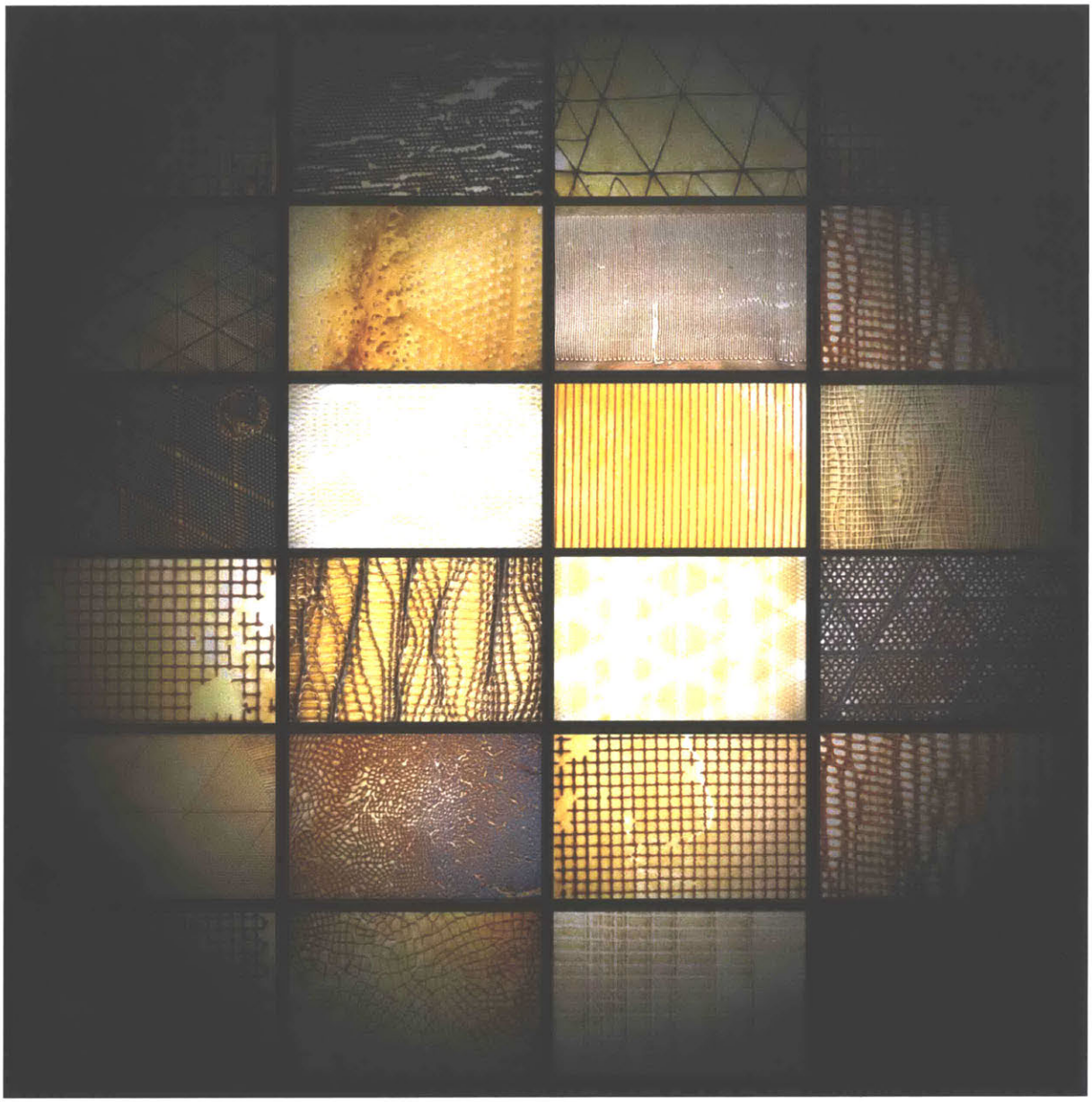

Figure 1.10 — Early experiments attempting to control mechanical and optical properties in skin-shell composites by tuning the chemical properties of hydrogels, resulting in tunable mechanical and optical properties of skins and shell patterns. Photo: Nicolas Lee.

Specifically, we were interested in how water landed on, was differentially immobilized by, got absorbed into, and evaporated out of the pectin skins because these features could be modulated to control how the contractile forces of the chitosan-cellulose lines would be resisted, stored as potential energy, or exacerbated. Practically, humidity and rain can land on a material, stay there, drip off, get absorbed, or evaporate away. In biopolymer-based materials, in particular, water retention and loss largely determine mechanical properties such as stiffness and conformation. While this phenomenon is not a new discovery, its utility in architecture has yet to be explored.

Immobilizing water in the forms of humidity and rain requires chemical or electrostatic attraction, or both. Thus, the chemical components and surface features of a pectin skin determine how water is sequestered from the atmosphere, stored, and utilized to do work. Moreover, PECs are generally permeable to all electrolytes, but impermeable to macroparticles.[15]

To investigate the surface features and hydrophilicity of the pectin skins used in Aguahoja I, we first ran 1 cm x 1 cm samples through an atomic force microscope (JPK Instruments NanoWizard 4a AFM) running in Quantitative Imaging (QI) mode to assess mechanical properties at 22°C and 65% relative humidity. The mapping resolution was set at 256 × 256 pixels and the scan size was between 10 × 10 μm^2 and 1 × 1 μm^2. The baseline was constantly updated to compensate for changes in the setpoint.

A non-contact cantilever (NCHR, Nano World, resonance frequency = 320 kHz) with a silicon probe was used to measure samples. Its stiffness was 60 nN and z-length was 50 nm. The pixel time was set to 12 ms, for repeatability. A polystyrene (2 GPa) test specimen (PS-LDPE-GS, Veeco Metrology Group) was used to fit the tip radius after running a specimen.

The five pectin skin compositions[14] as well as their corresponding surface features and elastic moduli are shown in Figure 1.10.

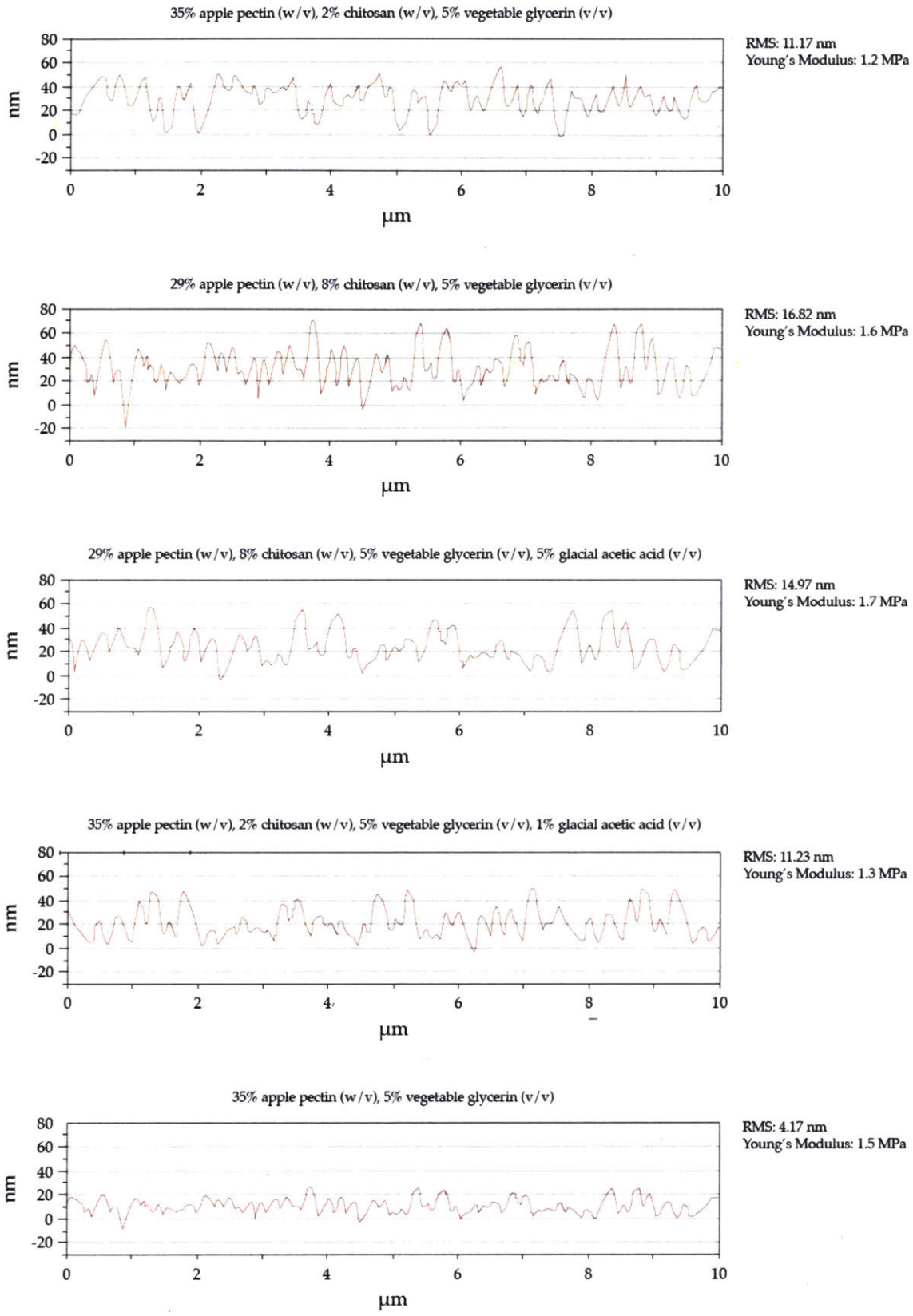

Figure 1.11 — Surface roughness measurements and elastic moduli of the five pectin skins used in Aguahoja I.

Contact Angle Hysteresis: Based on this information, the logical hypothesis was that a rougher surface would have more friction if a water droplet were to land on it. We tested this hypothesis by evaluating the contact angle hysteresis (CAH) of a water droplet on a tilted surface, using a VCA Optima video contact angle system (AST Products, Inc., Billerica, MA). We also tested the modulatory effects of new ionic groups on the surface features of these pectin skins, calcium carbonate, xanthan gum, alginate, casein, and titanium dioxide were used as fillers for the 35% pectin (w/v), 5% vegetable glycerin (v/v) skin.

In general, adhesive forces between a liquid and solid make a liquid droplet spread over a surface. Conversely, cohesive forces within the droplet cause it stick together and avoid surface contact.[16] A contact angle (CA) is the angle at which the adhesive and cohesive forces equilibrate, as a liquid-vapor interface meets a solid-liquid interface. Accordingly, a CA of 0° indicates perfect wettability; a highly wettable surface will have CA between 0° and 90°; a hydrophobic surface will have a CA between 90° and 180°; and a non-wettable surface will have a CA of 180°.[16] CA is defined by Young's relation, as follows:

$$\cos\theta_Y = \frac{Y_{LV}}{(Y_{SV} - Y_{SL}}$$

Where Y_{LV}, Y_{SV}, and Y_{SL} are the liquid-vapor, solid-vapor, and solid-liquid interface energies that result from adding up all the capillary forces acting on the line of contact and equating them to zero. However, this relation assumes a perfectly flat, rigid surface. A droplet on a real surface will deform due to surface curvature, surface roughness, the free energy of the droplet, ambient temperature, humidity, Laplace pressure, and a host of other factors. Thus, an equation relating the contact angle θ to the thermodynamics of the bulk material as well as the energy at the three-phase contact boundary and the surface curvature can be described as follows[17]:

$$\cos(\theta \mp \alpha) = A + \frac{B\,(\cos\alpha)}{a} \pm C\sin(\theta \mp \alpha)\,(\cos(\theta) + 1)^2 \left(\frac{(\sin(\alpha)\cos(\alpha) + 2)}{(\cos(\alpha) + 1)^2} \mp \frac{(\sin(\theta)\cos(\theta) + 2)}{(\cos(\theta) + 1)^2}\right)$$

Where the constants A, B, and C are defined as

$$A = \frac{Y_{SV} - Y_{SL}}{Y_{LV}}, B = \frac{\kappa}{Y_{LV}}, \text{ and } C = \frac{Y}{3Y_{LV}}$$

This equation assumes uniform curvature and a homogeneous surface. The Cassie-Baxter equation describes the arc angle of an equilibrated water droplet on a heterogeneous surface, as follows:

$$\cos(\theta^*) = r_f f \cos(\theta_Y) + f - 1$$

Where r_f is the roughness ratio of the wet surface and f is the fraction of surface area covered by a liquid.[16]

Importantly, the two equations mentioned above only consider differential deformation of a droplet due to environmental and interfacial factors; they do not consider the movement of a droplet along a rough surface, or the contact angle hysteresis (CAH).[18] Hysteresis is a an indication of how much liquids stick onto a surface, and is defined as the difference between the advancing and receding arc angles of a droplet moving along a surface, as follows:

$$CAH = CA_{adv} - CA_{rec}$$

If the contact angle at the front of the droplet, CA_{adv}, is greater than the receding angle, CA_{rec}, then the droplet will flow along the surface, in the direction of the advancing angle.[18] A small contact angle hysteresis indicates little resistance to the motion of the droplet due to surface roughness. High contact angles indicate increased contact between the surface and water droplet.

Ultimately, hydrophilicity has to do with a solid's outermost chemical groups.[19] In surfaces with similar structures, like our pectin skins, differences in wettability are due to differences in atomic packing. For instance, using a new ionic group to create branched chains between pectin and chitosan will induce poorer packing than in a surface with straight chains. A lower critical surface (Y_C) tension makes a material surface less hydrophilic.

Moreover, the pectin skins are low-energy surfaces because their liquid-vapor tension (Y_{LV}) is low and the bonds that hold them together (e.g, hydrogen bonds and van der Waals forces) are relatively weak and easy to break. Thus, they generally permit either partial or complete wetting. Interestingly, given that the mechanical properties of these skins change so much in response to temperature and humidity, they can be considered dynamic surfaces. This suggests that they undergo significant changes in surface energy when prompted by a given stimulus, which means that their hydrophilicity can be tuned through chemistry and environmental conditions.[14]

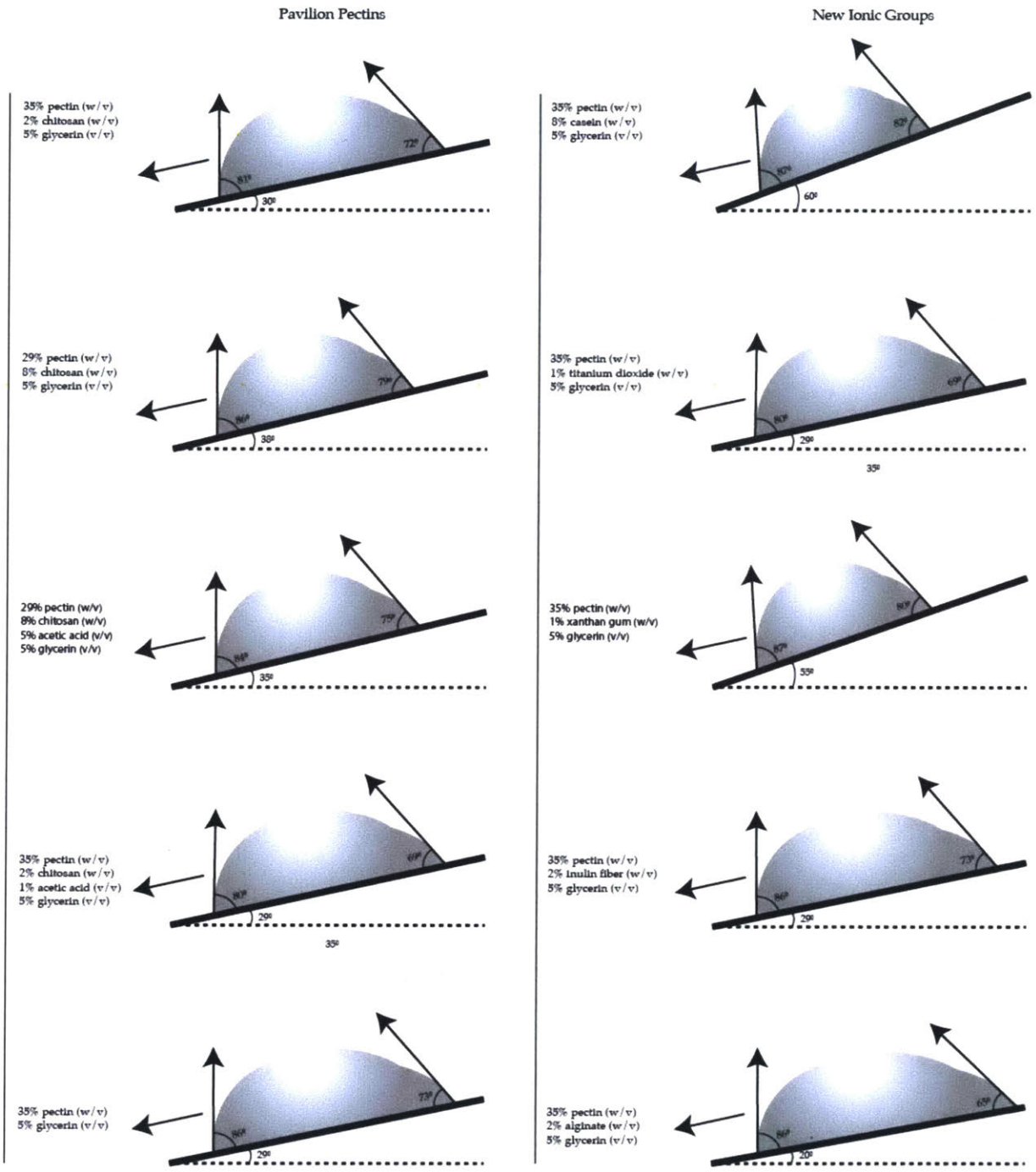

Figure 1.12 — Contact angle hysteresis (CAH) of the pectin skins used in Aguahoja I as well as a new set of skins with added ionic groups.

Here, adding in casein and xanthan gum dramatically increased the tilt angle, while adding alginate and inulin fiber from banana peels significantly decreased it. Thus, the addition of ionic groups from other organic waste streams to basic polyelectrolyte complexes could tune the hydrophilicity of pectin skins. In Aguahoja I, this was important because a pectin skin that could take up more water from the atmosphere would maintain flexibility after the chitosan-cellulose shell material had been printed onto it; whereas, one that was less hydrophilic would become more rigid and brittle at ambient conditions. A greater loss of water over time would cause more shape deformation and elasticity, while those that absorbed less water would be more brittle.

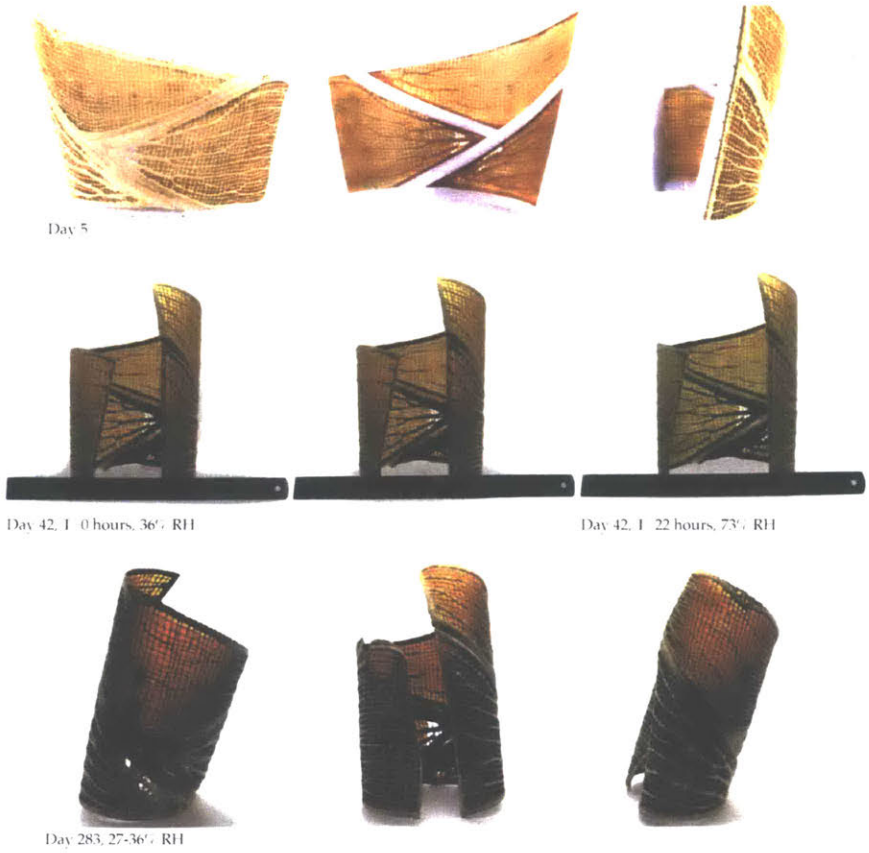

Figure 1.13 — Shape change of skin-shell composites over time and through a range of ambient relative humidity. Photo: Andrea Ling.[20]

These phenomena are important in architecture because they point toward buildings that will one way respond to heat and humidity to passively thermoregulate. Specifically, shape change and evapotranspiration can enable dynamic environmental responsiveness that is controlled via material chemistry, computational design, and digital fabrication. As opposed to an air conditioning system, these materials do not require energy input or digital control.

However, material chemistry and properties can only be useful in a building if contextualized within a hierarchical design and finely tuned during the fabrication process. Computational design was an incredibly useful tool toward this end because it enables several parameters to be considered in a generative design process. Therefore, simulation and fabrication information modeling (FIM)[21] became a framework through which to drive design generation with material chemistry, environmental conditions, fabrication parameters, and ecological function.

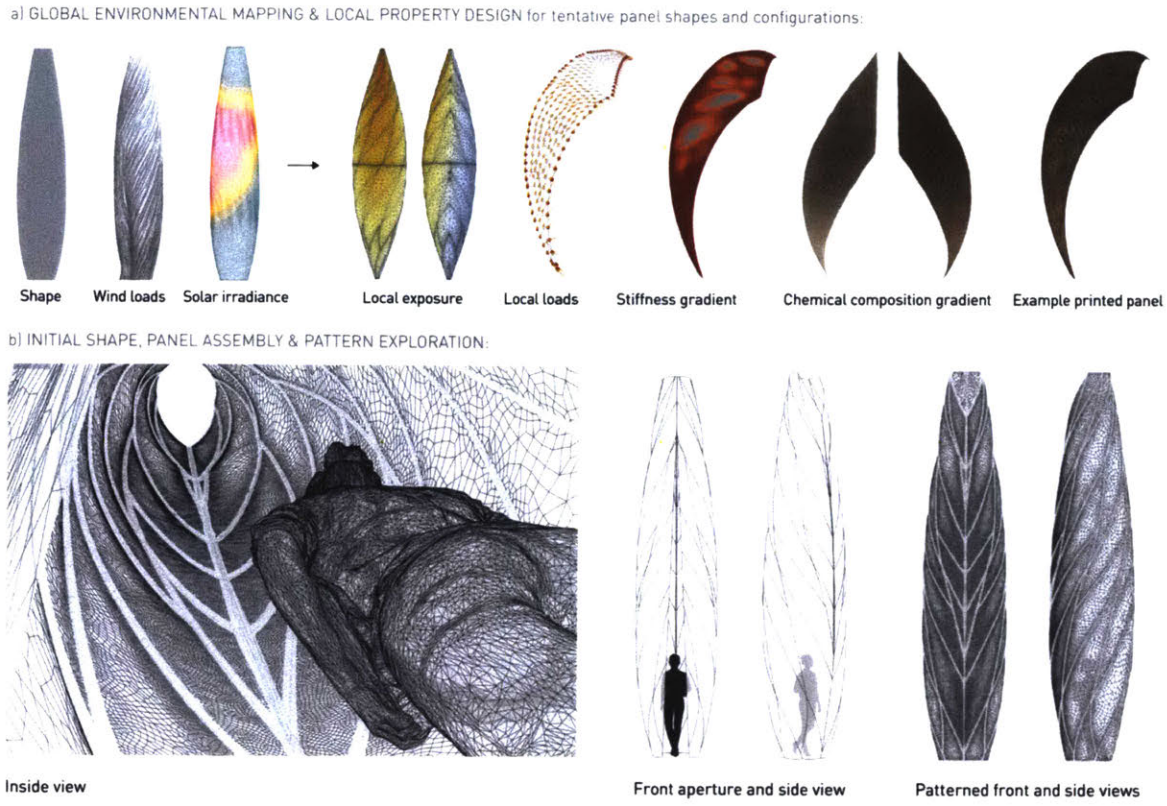

Figure 1.14 — A computational approach to generative design incorporating material properties, environmental conditions, fabrication parameters, and ecological function. Photo: Christoph Bader.[2]

Biologic Augmentation: After the pavilion had been put together, I attempted to further modify these water absorption and sweating behaviors by growing nature's gaseous air pollutant and humidity sponge[22], moss, in pectin hydrogels. Moss only needs moisture and sunlight to grow, and their growth can be revived at any time, making them ideal modifiers of ecofunctional infrastructure.[23] While miscroscopy showed that the moss could live in the dried panels, further research is needed to prove that this is a worthwhile path to follow.

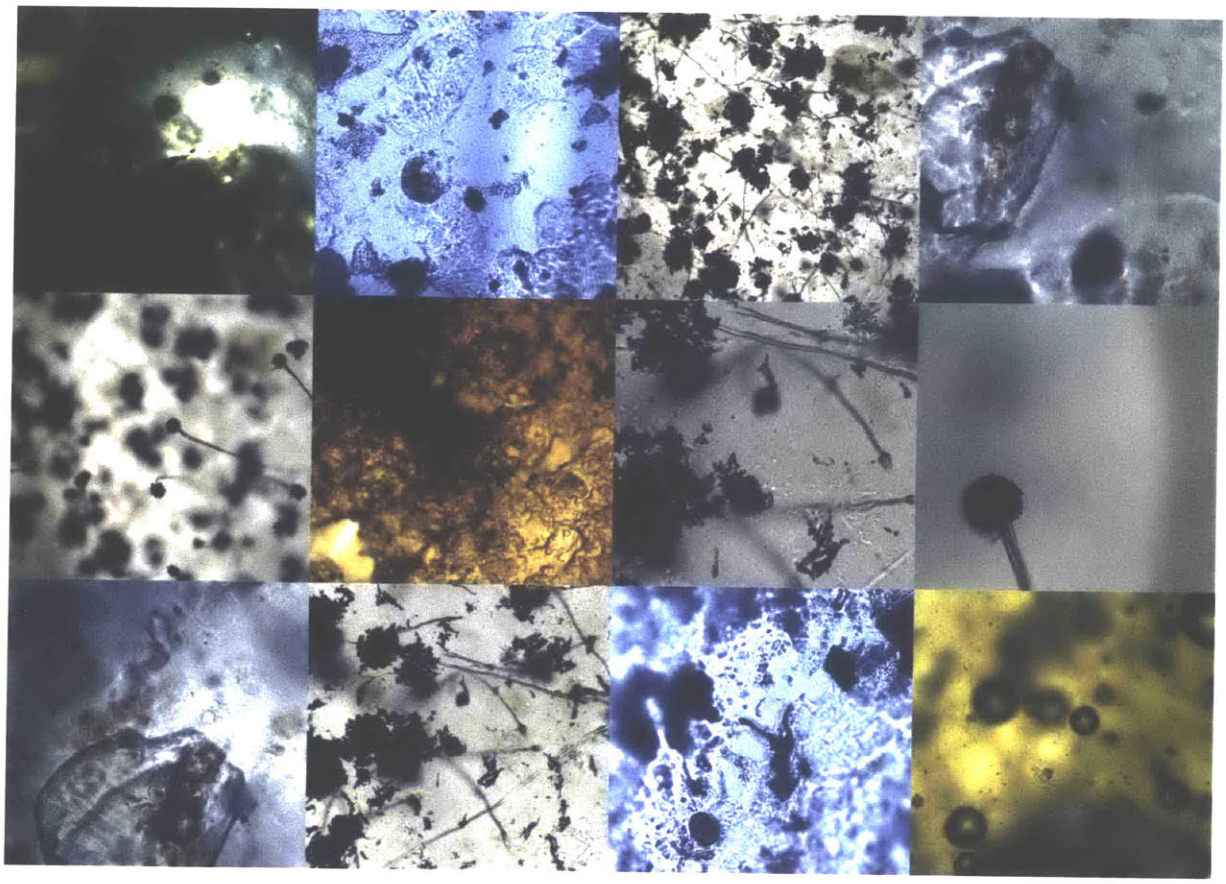

Figure 1.15 — Moss growing inside dried pectin films. Magnification: 4x. Photo: Nicolas Lee.

1.4 Ecofunctionality

The panels' rate of dissociation in water was an important design parameter in the pavilion. In short, infrastructural symbionts derived from organic waste streams should return to the resource cycles they came from.[20] To an extent, dissociation rates can be controlled with the aforementioned tricks enabled by polyelectrolyte chemistry. In particular adding in new ionic groups that lessen ionic strength and extend polymer chains is an effective tactic through which to achieve this goal.

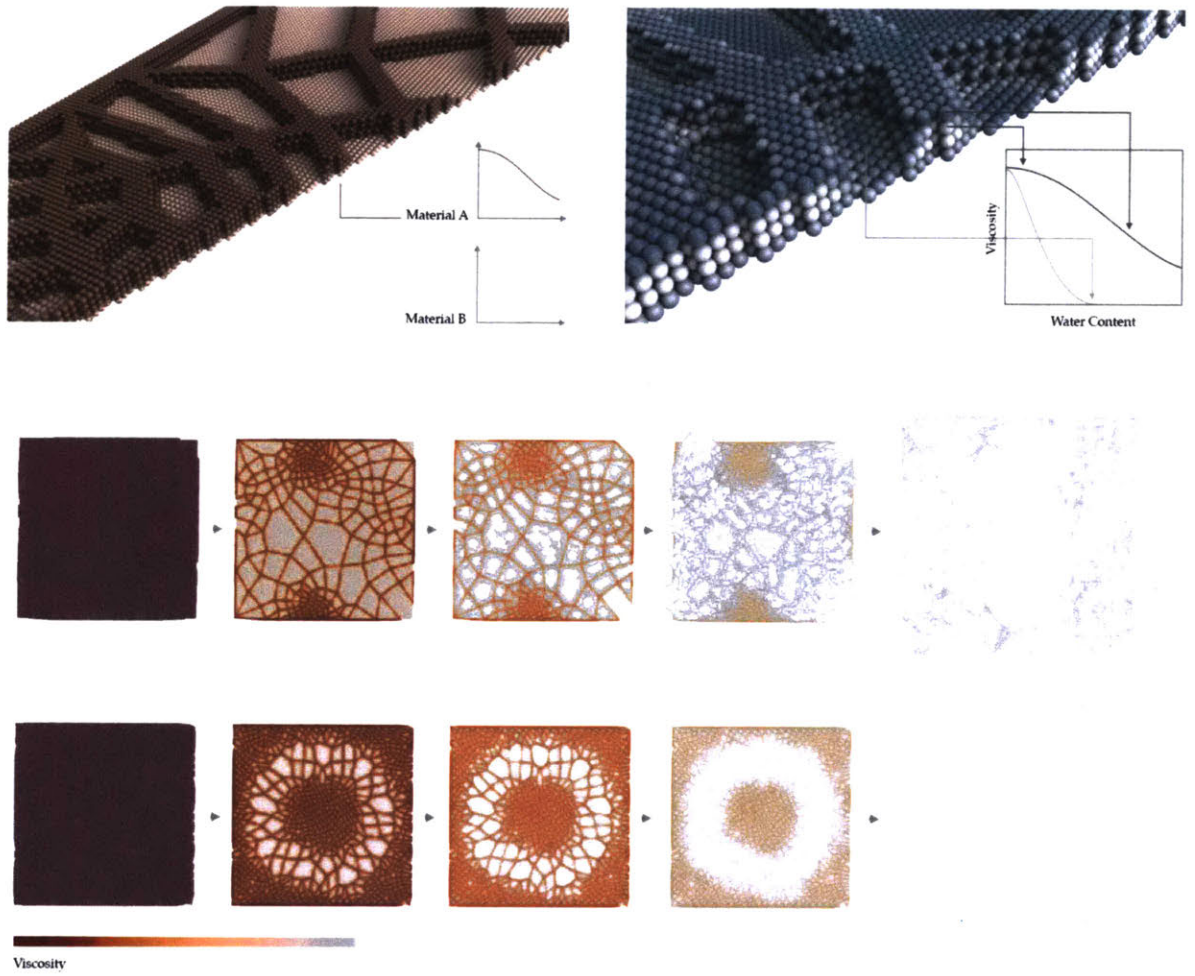

Figure 1.16 — Simulation of water-induced dissociation in samples with varying material distributions.[24] Photo: Andrea Ling.

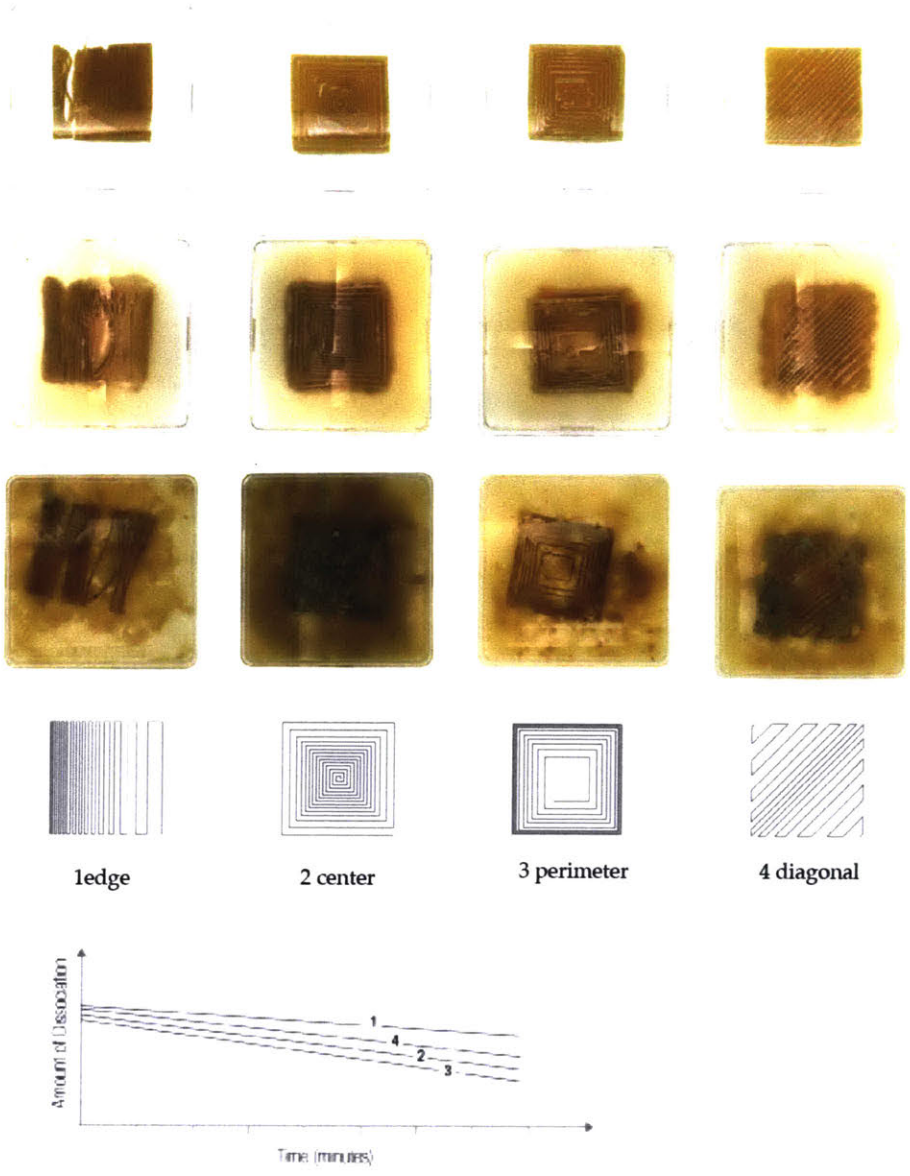

Figure 1.17 — Effects of material distribution in samples with equal mass on dissociation in water.[20] Photo: Andrea Ling.

Figure 1.18 — Water-induced dissociation of maquettes in high humidity, over a period of 25 days.

Figure 1.19 — Water-induced failure of maquettes in high ambient temperature and relative humidity, over a period of 20 days

1.5 Conclusions

Will these materials ever be used in buildings or products? Absolutely not. They are brittle, change from batch to batch, somewhat unpredictable, and do not last for a long enough period of time to be used as materials for buildings or products. However, the process of designing and evaluating materials in terms of their ecofunctionality is a valuable theoretical framework that I hope to advance in my future research.

Part 2 — Aguahoja II

2.1 Rationale

The second pavilion in the Aguahoja series expanded upon the computational design, material, and fabrication research undertaken during the creation of Aguahoja I, with much greater emphasis being placed on how aesthetic complexity within panels could be achieved through data-driven design. Within the hydrogels, viscosity and spread function became increasingly important parameters to modify to enable chromatic gradients that differentially bled into each other during the printing process. To do so, the following common kitchen ingredients were used as colorants:

1. Beet root
2. Green spirulina
3. Blue spirulina
4. Matcha powder
5. Turmeric + sulfur
6. Pink pitaya
7. Titanium dioxide + calcium carbonate
8. Squid ink
9. Pandan leaf
10. Mustard seed
11. Cinnamon
12. Chitosan (to modulate opacity and rigidity)

Although the rationale for doing so was more artistic than functional, I would like to think that as a reader scrolls through the following images presented in this chapter, he or she will think about how the skins are beginning to look like those of real animals. This is important because living things have evolved to respond to specific colors on other living things. These

can indicate changes in the environment, the existence of a nearby food source, impending danger, or the presence of potential mates, among other stimuli.

Incorporating other sensory stimuli — such as smells and surface textures coming from the colorants — can facilitate the creation of an ecofunctional language through which to communicate with and coordinate the behaviors of other organisms that occupy specific niches within an ecosystem. This again takes advantage of our abilities to conceptualize and design complex systems, while a majority of ecosystemic functionality has so far developed out of disparate pockets of necessary behavior.

Figure 2.1 — Closeup of the Aguahoja II skins. Photo: Ramon Weber.

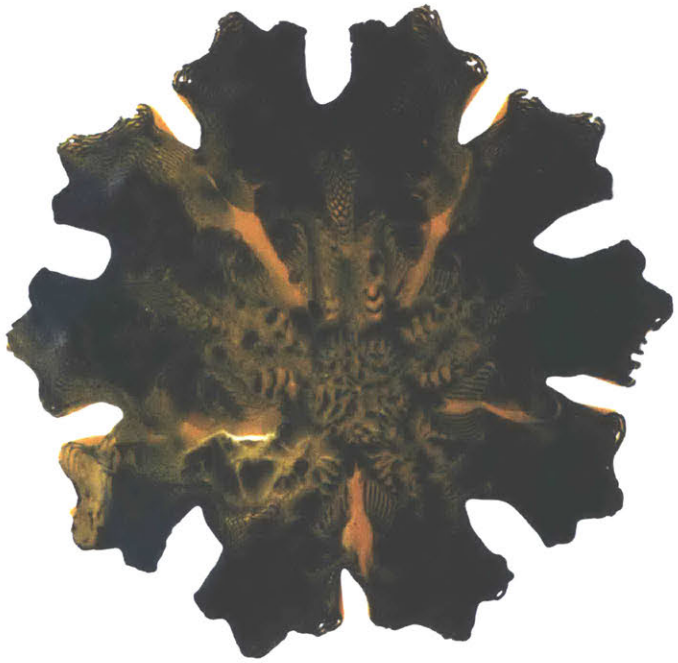

Photos: Joe Kennedy.

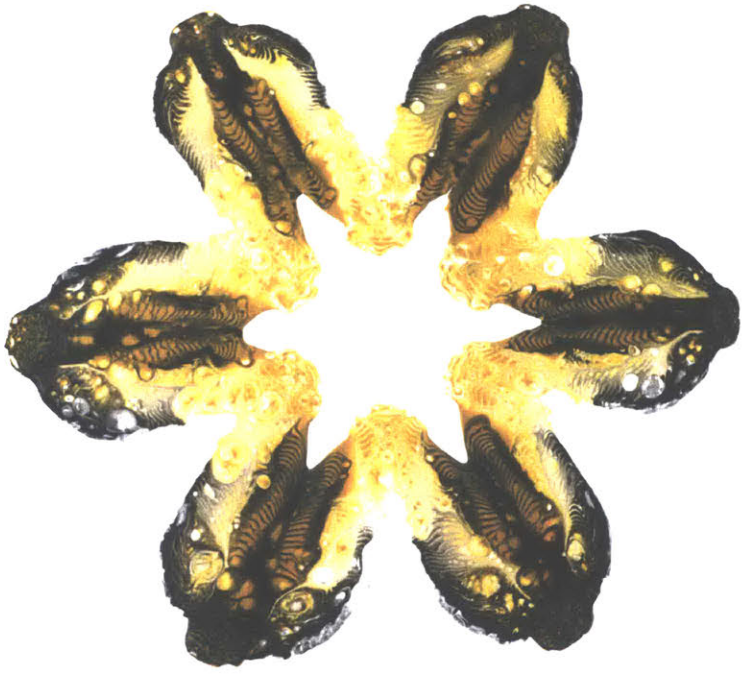

Photos: Joe Kennedy.

Photos: Joe Kennedy.

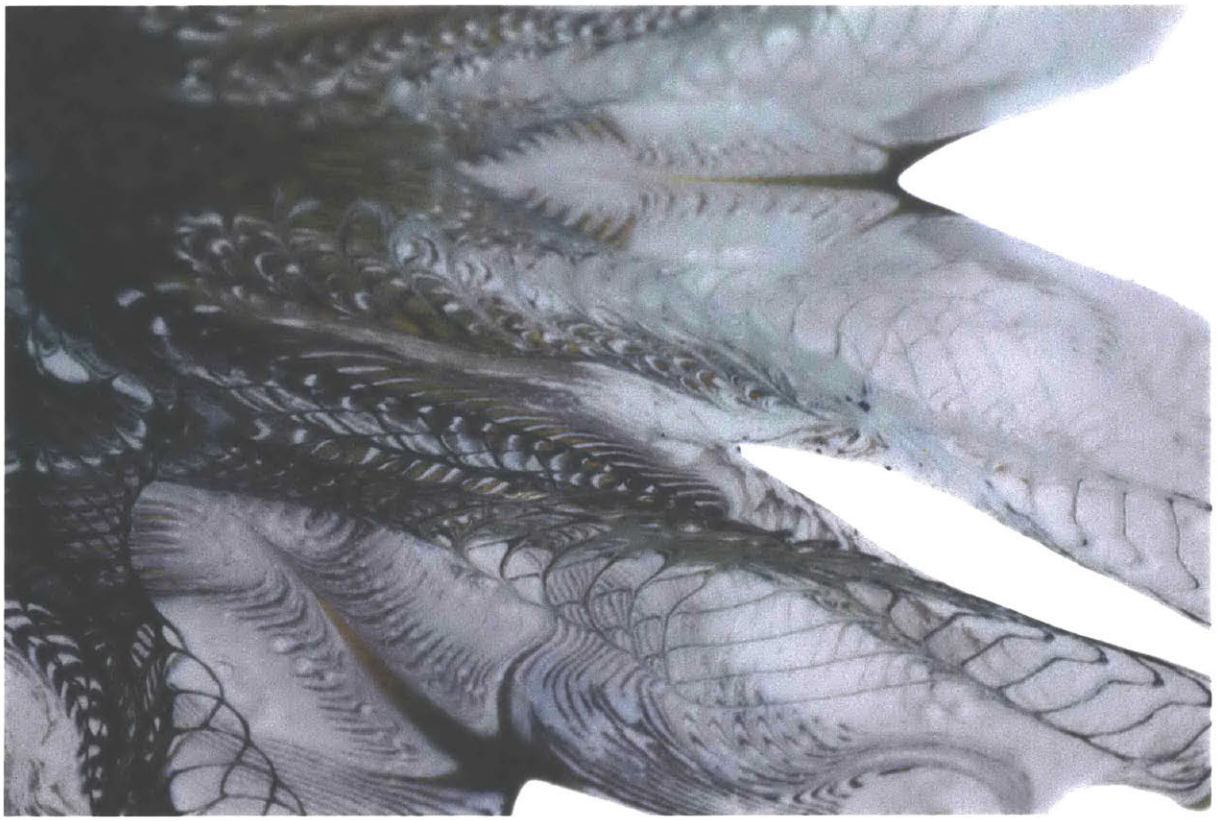

Photos: Joe Kennedy.

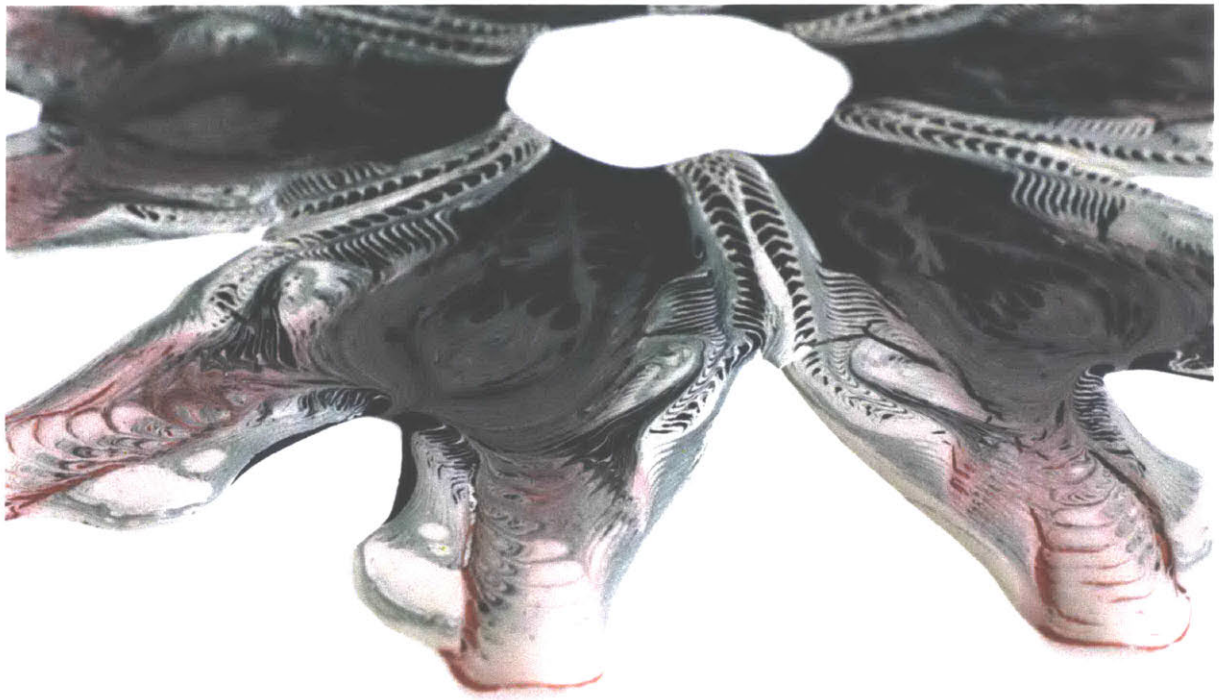

Photos: Joe Kennedy.

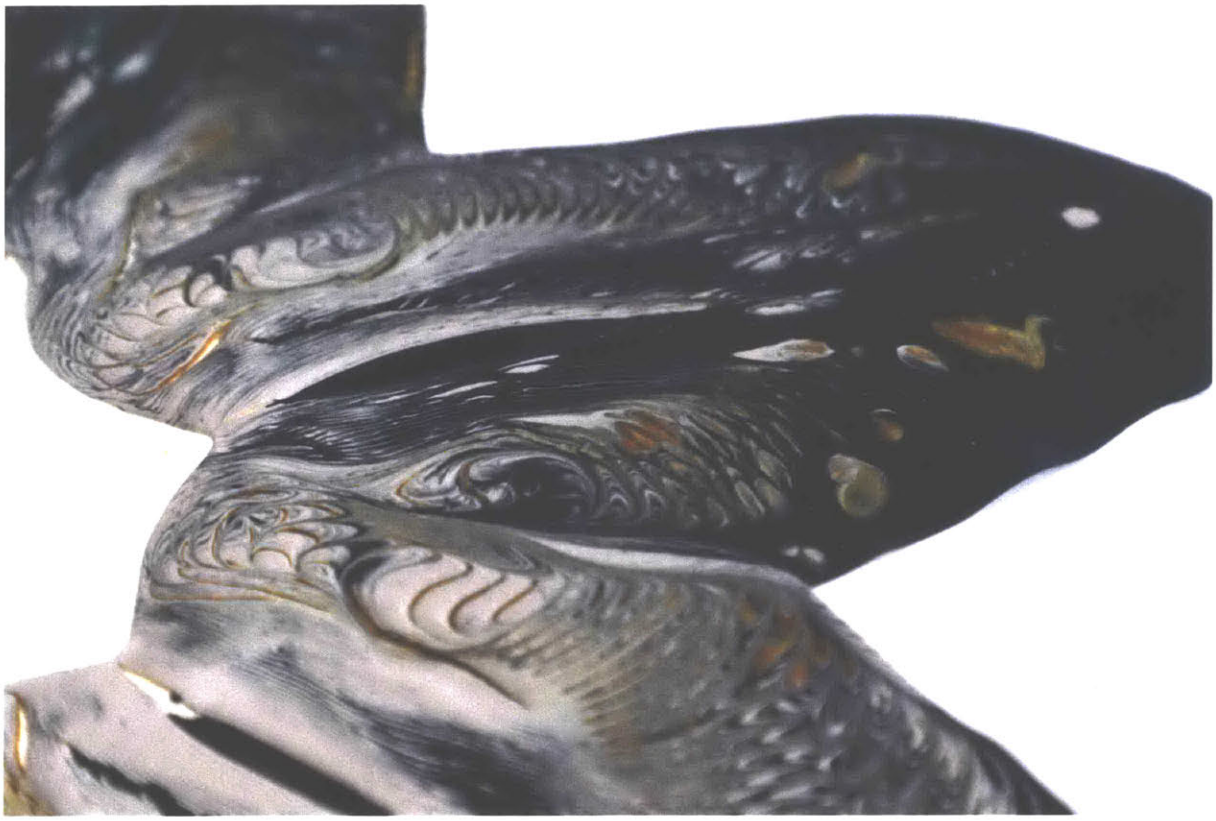

Photos: Joe Kennedy.

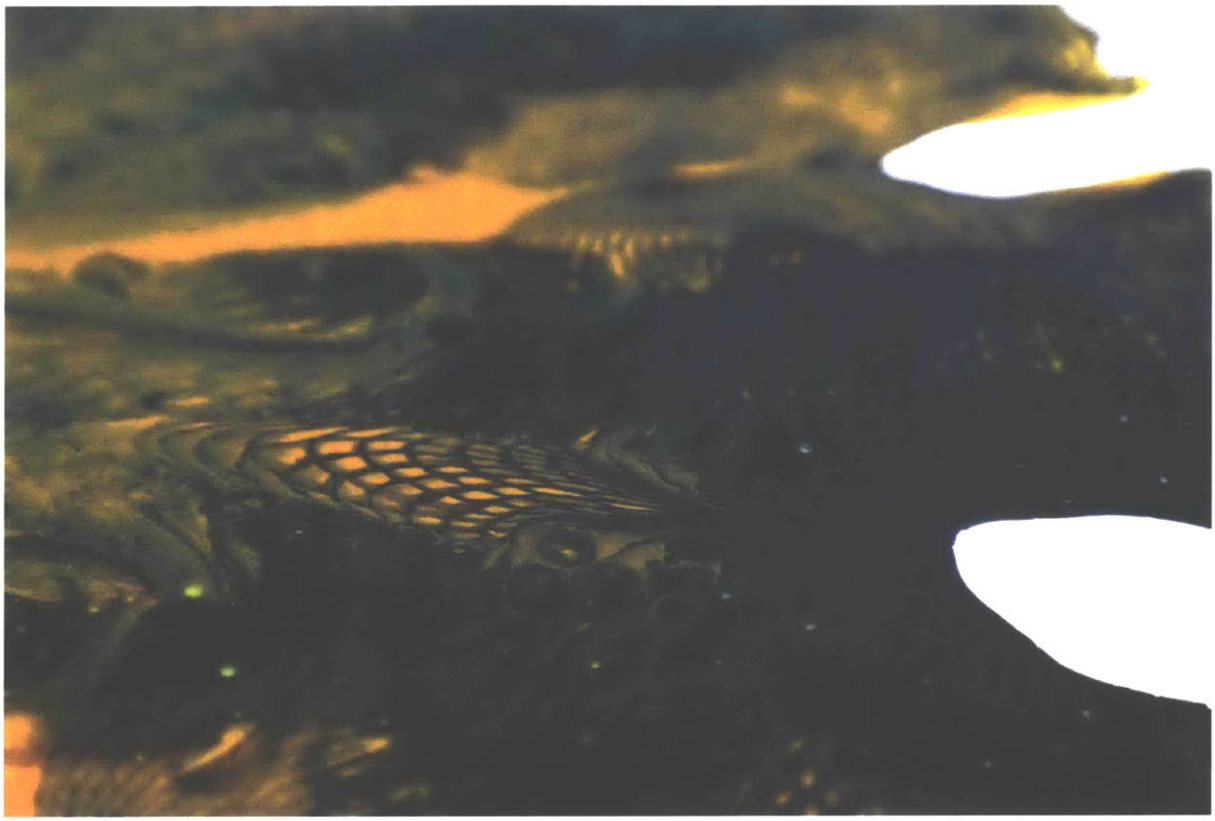

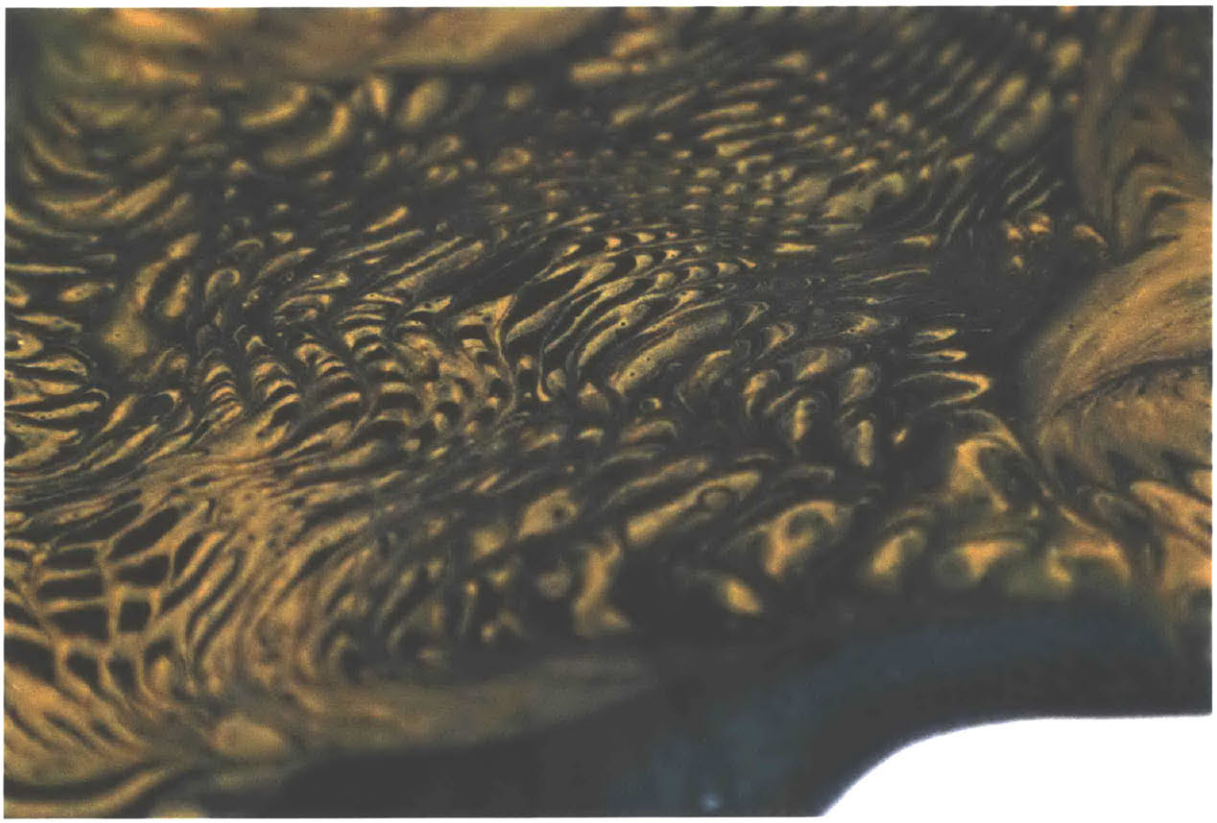

Photos: Joe Kennedy.

2.2 Conclusions

I have put this project into my thesis because it is suggestive of communicative infrastructure that may one day materialize in our habitats. While it is apparent that the skins have gained some complexity in the process of experimenting with colors, scents, textures, and gradients, I am really excited about applying this logic of functional gradation to growing building materials using workable cell lines, as can be seen in Part 3 of this thesis.

Part 3 — Opportunistic Chimeric Design

3.1 Rationale

The utility of Nature's most powerful capabilities is entirely context-dependent. Adaptations themselves are neither good nor bad; they just have a magnitude. Using this logic, bone cancers are ideal fabrication systems with which to co-create ecofunctional infrastructure because of the overpowering abilities they have developed through millions of years of evolution. To name a few, they create and repair massive, functionally graded structures; outmaneuver our most powerful immune responses, environmental extrema, and drugs, with minimal resources; and remodel their extracellular environments (ECMs) to optimize their proliferation and material production.

As an engineering material, bone — including cartilage, tendons, ligaments, muscle, and fat — is a lightweight structural material with excellent fracture toughness and fatigue resistance, as well as an ability to self-heal and dynamically respond to different loads. Therefore, engineers have attempted to mimic bone for a variety of products and structures.[25,26] However, the derivation, fabrication, and degradation of such mimics are both unsustainable and hard to control at the design resolution that makes bone so resilient. Thus, I have chosen to engineer osteosarcoma (ATCC® CRL-1547™, MNNG/HOS CI #5) and chondrosarcoma (ATCC® CRL-7629™, Hs819T) cell lines to grade between hard bone and soft, elastic cartilage, respectively, to gain access to nature's design palette and fabrication machinery. These specific cell lines were chosen because they were deemed to be suitable for transfection and proliferated quickly.

Doing so requires engineering both the cells and their environment across multiple time and length scales. At the genome level, I have stably transfected genes involved in proliferation and material production to maximize and speed up the material output of each cell line. With respect to the cells' environment, I have created programmable hydrogels using sensor cocktails, mechanical and gas diffusion gradients, and embedded chemical and electrical signals to influence the cells' density, growth direction, movement, and growth rate.

The ultimate goal of this project is to demonstrate a promising set of techniques and fabrication agents with which to grow ecofunctional materials and structures that participate in the construction and maintenance of their habitats, and degrade back into the resource cycles they came from after they have served their purpose.

3.2 Introduction

The most impactful adaptations in natural history have been motivated by extreme poles of competition and cooperation. Many of our most powerful technologic innovations, for example, have been developed to inflict massive damage in order to gain power and resources. However, adaptations are simply attributes or mechanisms that enable organisms to outcompete or outcooperate those with less optimal ecological fitness, and often benefit from millions of years of trial and error. As such, the context in which they are expressed can transform a competitive capability into one that is mutualistic — the constant here being the magnitude. This suggests that precisely designing the context in which nature's most powerful advancements are produced, expressed, and evolved can dramatically enhance our own fitness within, and the overall functionality, of our ecosystems.

For instance, the same capabilities that enable tumors to be so destructive inside a body actually make them ideal co-designers and co-fabricators of our habitats. Theoretically, the only constraints on tumor growth should be the availability of resources, vasculature, and structural integrity. Their robust mechanical properties, quick and effective adaptiveness, and infinite growth in resource-limited conditions may enable them to be more effective engineers and builders than our most sophisticated construction companies.

Specifically, osteosarcomas make hard, mineralized bone, while chondrosarcomas synthesize cartilage. Gaining control over these cells' micro-scale geometry, material distribution, and density can enable the creation of strong, lightweight cellular solids[27] and structures that not only outperform the best of our current building materials, but also heal themselves, kill surface-adherent pathogens, thermoregulate, and harness energy.

There are many potential benefits in doing so. At the ecological scale, growth of entire buildings can be executed by self-replicating cell lines, rather than diverting natural resources from our habitats faster than they can be replenished. At the building scale, quiescent cells living in the structure can be triggered to heal it when harmed or degrading; synthesize digestive enzymes to turn waste into energy; responsively modulate the structure's properties

to thermoregulate; mass-produce antibodies to kill surface-adherent pathogens before they infect us; and even one day coordinate thought processes to control these capabilities and evolve new ones. In other words, designing the fabrication technology and primordial environment that direct the growth and evolution of cancer cells can actually help heal our planet and protect us from diseases, and even enable aesthetic detail and complexity that cannot be achieved using other manufacturing processes.

Logistically, there are four dimensions of programmability involved in the designed biogenesis of materials: genes, environment, fabrication, and time. If environmental signals can be spatially, temporally, and hierarchically organized to precisely direct cancer cells to grow along specific pathways, aggregate or metastasize on command, and alter their material products, the resulting structures may realize a design intent with high fidelity. However, cancer cells change and are changed by their environment. For instance, a single cancer cell will undergo a multitude of genetic and transcriptional changes during one experiment in a lab setting, such that all populations derived from it are genetically heterogeneous.[28] This fourth dimension of constant dynamism makes controlled fabrication both challenging and potentially more rewarding than traditional manufacturing techniques.

Living cells can simply do more than the polymer chains that comprise plastics or even biologically derived materials. Moreover, given that there has been so much research and funding devoted toward cancer, doctors and scientists have developed our most advanced and thoroughly validated tools for directly imaging and manipulating specific cell lines and their material products. Our greatest capabilities are brought out when the stakes are highest.

3.3 Background

Biofabrication is a relatively new field, with ancient origins. Its defining characteristic is, perhaps, complexity. Normally, extreme care is taken to grow cells in a material system – usually, a hydrogel or scaffold – that accurately recapitulates their native physiologic environment. As such, artificial ECMs are essentially programmable media used to talk directly to cells. Physical properties such as pore size, network geometry, stiffness, surface roughness, and viscosity are the primary mechanical means through which cells decipher when to proliferate, aggregate, migrate, and differentiate. In addition, these signals impact how cells specifically alter their extracellular matrices (ECMs) to grow, self-organize, and sustain themselves.

A cell must be able to move through a biocompatible gel or scaffold by enzymatically breaking noncovalent bonds. At the same time, the gel or scaffold has to remain hydrated and structurally stable to support the material products and cellular aggregates forming within it. Thus, pore size has to relate to both the cell diameter and tissue morphology.[29] Due to their stretchable actin cytoskeletons, osteosarcomas and chondrosarcomas utilize complex mechanotransduction signals in response to traction forces from their surroundings to synthesize and secrete specific enzymes and other ECM components to optimize their growth environment and create tissue.[30] Thus, polymer chains must have adhesive proteins and proteoglycans that each cell type can recognize and attach to.

Moreover, specific signaling factors are secreted to coordinate responses from other cells regarding when conditions are sufficient to grow into tissues. Out of necessity, this process includes the production and recruitment vasculature for nutrient delivery. Finally, the meso-scale network architecture and topography must direct these cellular aggregates to produce the desired tissue geometry, while also ensuring the cells stick to the right places and can release themselves should they need to migrate via diffusion and/or affinity.[31]

Beyond pure mechanics, fields, forces, and flows of chemical metabolites, ions, growth factors, gases, drugs, and other signals must be topologically templated in order to engage cells in

specific feedback loops.[32] In turn, cells, especially cancer cells, initiate conditional epigenetic responses by altering their own physiology, that of their neighbors, and/or the makeup of their ECMs. Furthermore, there are multiple ways in which cells can aggregate, from sheets to spheroids and everything in between, which largely dictate the type of material system produced, its geometric and mechanical properties, and the extent to which large-scale tissues can be created. Crucially, environmental remodeling and recruitment of somatic cells enable tumors to commandeer vasculature to ensure a constant supply of nutrients, especially as they grow larger and more heterogeneous.[33]

Here, fabrication methods come into play. Bioprinting is a layer-by-layer extrusion process that enables multiple materials and cell types to be spatially distributed, based on information from a design file, within a printed structure. However, given that there are so many parameters to consider in such a process, many complexities can either be detrimental or exponentially beneficial to such a fabrication process.

Depending on how long and under which conditions the cells are cultured — i.e., whether they are grown as spatially separated individuals or coerced into other types of aggregation — as well as how many cells are extruded per unit volume in an additive manufacturing process, vastly different aggregate geometries, materials, and material properties will result. Moreover, depending on the force with which cells are secreted through a nozzle with a particular diameter or the extent to which an extrusion nozzle disrupts an already printed network, cells may not live through the fabrication process.[34] If the cells do live through the process, they, along with their signaling factors, should remain at or near the spot of deposition until prompted to move.

Even often-overlooked logistics such as freezing cells in the right type of liquid, for an appropriate amount of time; handling and printing the cells carefully, without puncturing or crushing them; giving them the right dosage of growth media; keeping only the cell types of interest in the scaffold or gel; and finding disruptive or complementary combinations of signaling factors can dramatically alter their viability and behavior.[35] In particular, the source

of any growth medium or matrix component can create unintended consequences based on misfolded proteins, cytotoxic degradation products, immune responses, and other unpredictable events.[36]

In addition, hydrogels alone cannot typically support complex, large-scale constructs, so some form of biocompatible support is usually printed or laid down.[34] This can confound all mechanical and chemical signaling factors programmed into the ECM. Factor in other cell types — each of which requires a different set and quantity of ECM properties, food, and signals — and these confounds will alter the behavior of all other cells in terms of complex functional gradation, hierarchical organization, vasculature, and epigenetic changes over time. Even after all of these considerations have been accounted for, this background survey only scratches the surface of biofabrication's complexity and potential.

3.4 Related Work

Genes: The first criteria that need to be satisfied in order to grow large structures using bone cancer cells are rapid reproduction and massive material output. One way to achieve these goals is to borrow from other structures that satisfy these stipulations. For instance, deer antlers consist of some of the fastest growing mammalian tissues. They are able to grow up to 2 cm per day and produce 10 kg or more of bone tissue within a 2-3-month period.[37]

Ker *et al.* (2018) found that Under identical culture conditions, deer antler reserve mesenchyme (RM) cells proliferated 8.6–11.7 times faster than and exhibited 17.4 times the calcium mineralization of human mesenchymal stem cells (hMSCs), paralleling in vivo conditions. Two key proliferation and mineralization genes in fallow deer, *uhrf1* and *s100a10*, played large parts in these abilities. Importantly, expression of each or both in hMSCs dramatically increased one or both parameters, respectively.[38] In tumor cells, *uhrf1* mediate the ubiquitination of key genes involved in tumor suppression and cell cycle checkpoints,[39] while *s100a10* encodes key calcium-binding proteins that are used to make bone.[40]

Environment: Aldaye *et al.* (2010) have pioneered a technique for creating structurally tunable DNA-based extracellular matrices that enable precise control over biophysical and chemical signaling effectors. DNA nanotechnology utilizes base-pairing to create predefined one-, two-, and three-dimensional structures that direct the growth of cells, organized the topology of proteins and nanoparticles, and facilitate diagnosis and drug delivery. These authors have combined tools and techniques from DNA nanotechnology with protein engineering to generate a new class of DNA/protein extracellular matrices that can parametrically control cell morphology, behavior, signaling, and transcription factor localization.[41]

Doing so also enables evasion of sourcing problems and imprecision in traditional hydrogel matrices that result from misfolded proteins, immune responses, and mechanical inhomogeneities. In short, knowing exactly what is in the environment one is designing is incredibly useful in such a complex process. Moreover, specific signaling factors, attachment

sites, pore sizes and lengths, proteins, and sensory mechanisms can be embedded in a DNA hydrogel, making it an incredibly useful tool for biofabrication.

In terms of scaling this system up, Park *et al.* (2009) have developed DNA hydrogels that are made entirely from DNA. In such gels, biologically relevant signaling factors can be easily encapsulated during enzymatic gelation, which is done in physiological conditions. Accordingly, their properties and immobilized signals can be tuned by adjusting initial concentrations and using different types of branched DNA monomers. This is perfect for controlled drug delivery, tissue engineering, 3D cell culture, cell transplant therapy, and other biomedical applications.[42]5/14/19 10:51:00 AM Here, a linear expression plasmid is incorporated into a DNA hydrogel by using branched DNA monomers as crosslinkers. The resulting P-gel is formed into sheets, which replace plasmid DNA during coupled transcription/translation in cell-free expression. The authors have gotten yields up to 5 mg/ml of protein in a single expression, which is significantly better than commercial solution phase systems.[43]

With respect to mechanical properties, Forget *et al.* (2017) have been able to tune the elastic modulus of printed gels over several orders of magnitude (5–230 Pa), almost independently of shear viscosity (10–17 mPa), by adjusting the degree of carboxylation in an agarose hydrogel. Using this carboxylation technique can enable spatially templated mechanical domains within 3D printed structures resulting from identical printing parameters and low nozzle shear stress.[44] By adding in beta-tricalcium phosphate (β-TCP), Sen *et al.* (2018) have been able to further stiffen carboxylated agarose to recapitulate the mechanical properties found in compact bone ECM.[45]

Signaling: To create gradients of oxygen levels and diffusion within mechanically tunable hydrogels, Park and Gerecht (2014) have fabricated a hypoxia-inducible hydrogel consisting of gelatin and ferulic acid, which consume oxygen to form hydrogel networks via a laccase-mediated reaction. Neoplastic cells such as osteosarcomas and chondrosarcomas growing under hypoxic conditions exhibit a more aggressive phenotype by activating chemical

cascades that are partially mediated by hypoxia-inducible transcription factor (HIF-1α) and vascular endothelial growth factor (VEGF) to ensure a constant nutrient supply. These conditions often prompt aggregation and densification of cellular aggregates, which can result in denser, stiffer material deposition.[46]

By substituting dextran for gelatin, the same lab was able to induce long-lasting hypoxic conditions (~12 hours), compared to those in the gelatin-based hydrogel (~1-1.5 hours). Given that hypoxic conditions must last for several hours to trigger downstream signaling pathways and facilitate relevant transcription factor accumulation, grading between the two gels may yield precise control over cellular aggregation and material properties.[47]

Beyond mechanical and gas diffusion manipulations, actual chemical and electrical messages must be embedded into hydrogel matrices in order to precisely direct the growth, aggregation, fusion, and material production of cells. Simply infusing such signals into a printed hydrogel, however, does not allow for spatiotemporal specificity or triggered release. Thus, some method of precisely templating and timing these signals must be incorporated into the hydrogel engineering and fabrication processes.

In particular, cellular aggregation to form larger tissues is very hard to achieve in a biofabrication processes. There is no reason, *per se*, that simply printing layer after layer of bone cancer cells will result in hierarchically organized, osteointegrated, functionally graded bone structures. Thus, Cheng *et al.* (2017) have created a gelatin-based hydrogel modified with a catechol motif and silicate nanoparticles to promote controlled local delivery of immobilized factors that enhance cell functions, direct new tissue formation, and promote bio-integration.[48]

Sensing and Reporting: As opposed to measurements of bulk properties, cells really care about nano-to-mesoscale properties in their immediate environment. However, such signals are difficult to localize and detect, and reporters often dissociate, sink, or diffuse away relatively quickly. Moreover, signals relying on light — for instance, sensors or fluorescent reporters of protein production — cannot get destroyed or interfere with one another via quenching, color redundancy, unintentional excitation, or other confounding events.[36]

Wu *et al.* (2010) have created a ratiometric, single-nanoparticle oxygen sensor for biological imaging. The system consists of π-conjugated polymers doped with an oxygen-sensitive phosphorescent dye. After one- or two-photon excitation, the polymer transfers energy to the dye, thereby producing bright phosphorescence that is highly sensitive to dissolved oxygen concentration. The sensors' small size, intense brightness, and ratiometric emission, as well as their capacity for single-particle sensing and cellular uptake, make them promising candidates for quantitative imaging of local molecular oxygen concentration.[49]

Du *et al.* (2017) have been able to quantitatively image pH in living cells and ECMs with a ratiometric probe based on upconversion nanoparticles that have been modified with a pH-sensitive moiety. With this system, the authors have done live cell quantitative imaging of properties and behaviors such as positive cellular uptake, biocompatibility, long wavelength excitation, and pH response within a biologically relevant range. Local pH gradients are important to detect in order to figure out how a given pH range, at a specific developmental age, both impacts cells and triggers modifications to the ECM.[50] For instance, Matsubara *et al.* (2013) have shown an additive influence of acidic local extracellular pH, low oxygen tension, and high pressure in the proliferation rate and metastasis of osteosarcomas.[51]

Similarly, temperature is correlated with all cellular events including cell division, gene expression, enzyme production and enzymatic reactions, metabolism, and pathogenesis. Uchiyama *et al.* (2015) have synthesized ratiometric fluorescent polymers (RFPs) via reversible addition–fragmentation transfer polymerization for intracellular and ECM temperature sensing within a biologically relevant range. The system consists of a thermo-sensitive polymer, polarity-sensitive fluorescent dye, and thermo-insensitive fluorescent dye. A high local temperature triggers increases in the fluorescent intensity of RFPs due to self-assembling of the thermo-sensitive polymer. Given the size of the particles, both temperature sensing and ratiometric imaging of temperature variations associated with biological processes can be captured using a standard digital camera.[52]

Histology must also be performed to evaluate cellular responses to these signals and verify that the right behaviors and products are being induced at the right times. To distinguish bone from cartilage, Rigueur and Lyons (2014) utilized Alcian blue and Alizarin red staining, respectively.[53] In addition, given that matrix metalloproteinase 2 (MMP-2) has been found to be associated with osteosarcoma and chondrosarcoma invasion and metastasis, Zhang and Zhang (2015) used PV 6000 immunohistochemistry to confirm its production by osteosarcomas *in vitro*.[30] This is one mechanism cells use to break a hydrogel's noncovalent bonds to move from one place to another.

In addition, it is useful to know when cancer cells are preparing to invade, aggregate, or metastasize. Zhu *et al.* (2013) incubated osteosarcoma cells with a primary SOX9 antibody and a secondary antibody using anti-mouse IgG, to which biotin was attached. Color development was done with hematoxylin contrast staining.[54] Gathering such data will inform which, if any, genetic manipulations are needed to speed up or direct growth direction and density in specific ways.

Fabrication: There are multiple ways in which hydrogel material can be laid down via additive manufacturing. Unsurprisingly, each has costs and benefits relating to how the technique differentially influences cell behavior and the structures they create. These parameters relate to which kind of force a printer uses to extrude materials, what happens to cells and the materials they are inside of upon making contact with the print bed and over time, and whether or not other materials, conditions, or cells modify these structures. Each new layer also introduces forces that displace the printed structure and the cells therein. Moreover, shrinkage and warping due to heterogeneously dispersed phase changes significantly limit the scale and resolution of printed constructs. These particularities dramatically impact cell growth and behavior.

Rocca *et al.* (2017) have dramatically improved the experimental setup for embedded extrusion bioprinting, which allows for complex structures that cannot be achieved with conventional layer-by-layer deposition by negating effects from the aforementioned forces and phase

changes. Using a rigid hydrogel bath as a sacrificial printing environment, a bioink is deposited and crosslinked within the bath in the form of a continuous stream or droplets. Upon completion, the resulting structure can be subsequently released from the hydrogel support. Combining this 3D bioprinting technique with a multimaterial extrusion printhead will enable complex, functionally graded structures built from multiple bioinks, which cannot be realized by conventional manufacturing processes.[34]

3.5 The Logistics of Growing Tunable Bone Structures

Genes: To grow large structures using cancer cell lines, one first needs many cells that produce a ton of material, in a short period of time. Thus, I stably transfected *uhrf1* and *s100a10* from fallow deer to increase the proliferation and mineralization, respectively, in osteosarcomas and chondrosarcomas. Since both cell types express *uhrf1* and *s100a10*, t wanted to investigate the impacts of overexpression on population growth and mineralization.[55,56,57,58]

The calcium mineralization-modulating gene *s100a10*, which encodes the S100 calcium binding protein A10, was stably transfected into the osteosarcoma MNNG/HOS CI #5 cell line using a pcDNA3.3-TOPO cloning vector, with a constitutive promoter. Neomycin-resistance and a mCherry fluorescent reporter at the C-terminus were encoded into the plasmid.

Additionally, the ubiquitin-like with pHD and ring finger domains 1 (*uhrf1*) gene was stably transfected into both osteosarcoma (ATCC® CRL-1547™, MNNG/HOS CI #5) and chondrosarcoma (ATCC® CRL-7629™, Hs819T) cell lines to constitutively upregulate the proliferation of each. An EGFP reporter was added to the C-terminus for microscopy and neomycin-resistance was encoded into the plasmid to indicate successful transfection. Each sequence was optimized for human cell line expression using Thermo Fisher's GeneArt Gene Synthesis service.

MNNG/HOSCI#5 (*s100a10*$^{+}$/*uhrf1*$^{+}$), (*s100a10*$^{+}$/*uhrf1*$^{-}$), and (*s100a10*$^{-}$/*uhrf1*$^{+}$) cell lines were created to test the effects of overexpressing each on the rates of proliferation and calcium mineralization. A Hs819T (*uhrf1*$^{+}$) cell line was created to investigate this gene's effects on proliferation. It is important to note that in the following text and figures, the terms *uhrf1*$^{+}$ and *uhrf1*$^{-}$ are used to indicate the overexpression of this gene, not its presence or absence in a cell line's genome.

Population measurements were taken using a TC20 Automated Cell Counter (Bio-Rad Laboratories, Hercules, CA) and calcium mineralization was evaluated using Alizarin red staining (Sigma-Aldrich 130-22-3, St. Louis, MO). The growth of each cell line was compared

to that of its wild-type counterpart. All cells were grown in McCoy's 5A Medium (Thermo Fisher Scientific #16600082, Waltham, MA), with 10% fetal bovine serum (Thermo Fisher Scientific, Waltham, MA), 0.5% antibiotic-antimycotic (100X) (Thermo Fisher Scientific #15240062, Waltham, MA), and 1% neomycin sulfate (Thermo Fisher Scientific #21810031, Waltham, MA).

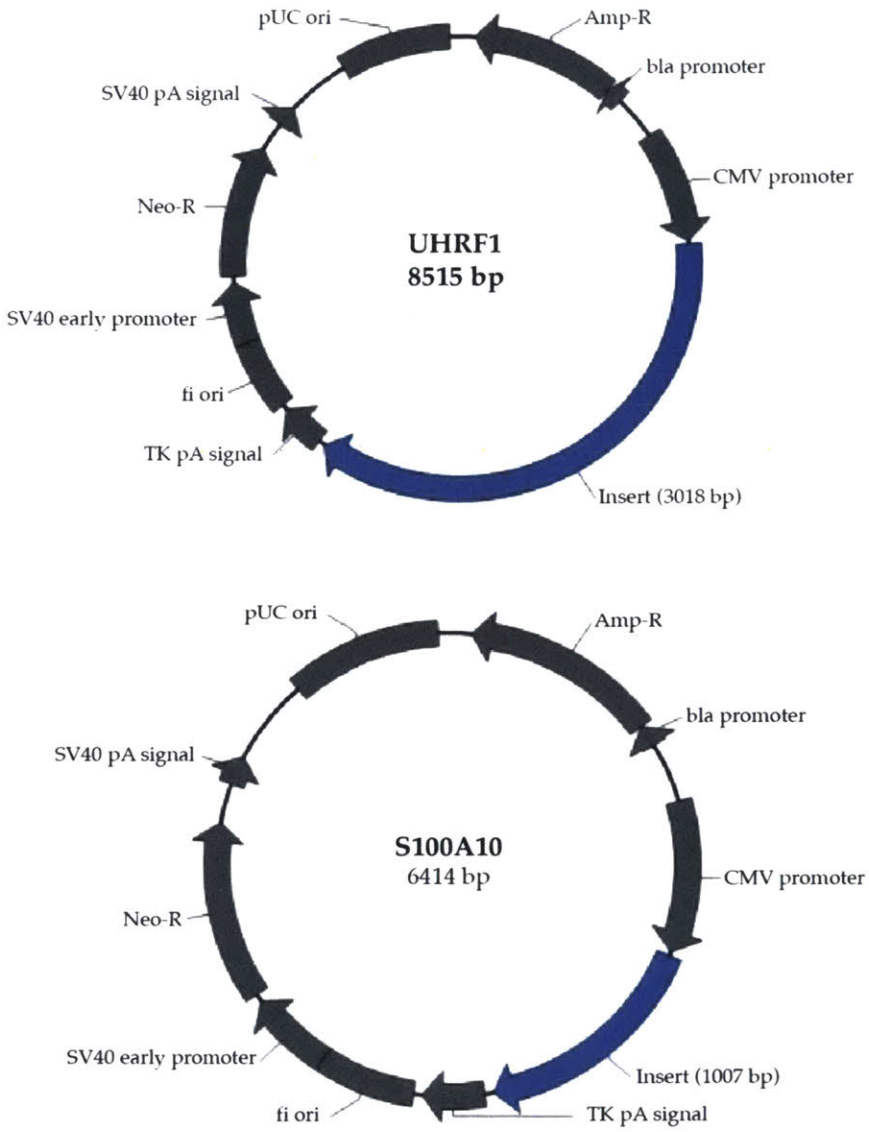

Figure 3.1 — *uhrf1* and *s100a10* plasmids. Photo: Thermo Fisher GeneArt Gene Editing service.

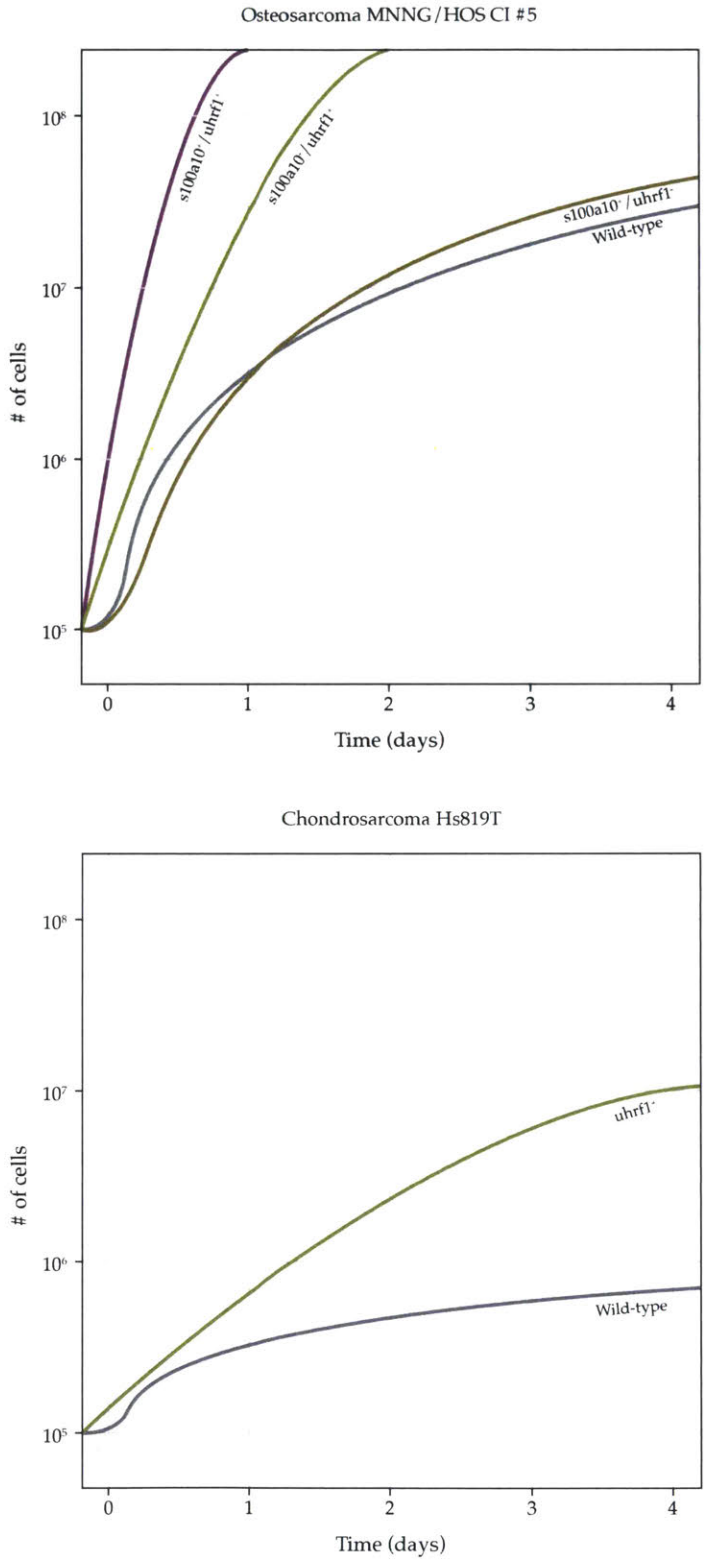

Figure 3.2 — Chondrosarcoma mutant population growth: wild-type vs. *uhrf1*⁺. The medium was changed every two days and all experiments were performed in triplicate.

Environment: Continuing the effort to maximize the amount of cells and material production over time, I next added various bioactive peptides (10 ng/ml),[59] each in a separate flask of growth medium, known to enhance the proliferation of osteosarcoma cells, to analyze population growth of osteosarcoma cells with and without *uhrf1*. In this experiment, I doubled the growth medium and started with fewer cells (10^4) to prevent overcrowding.

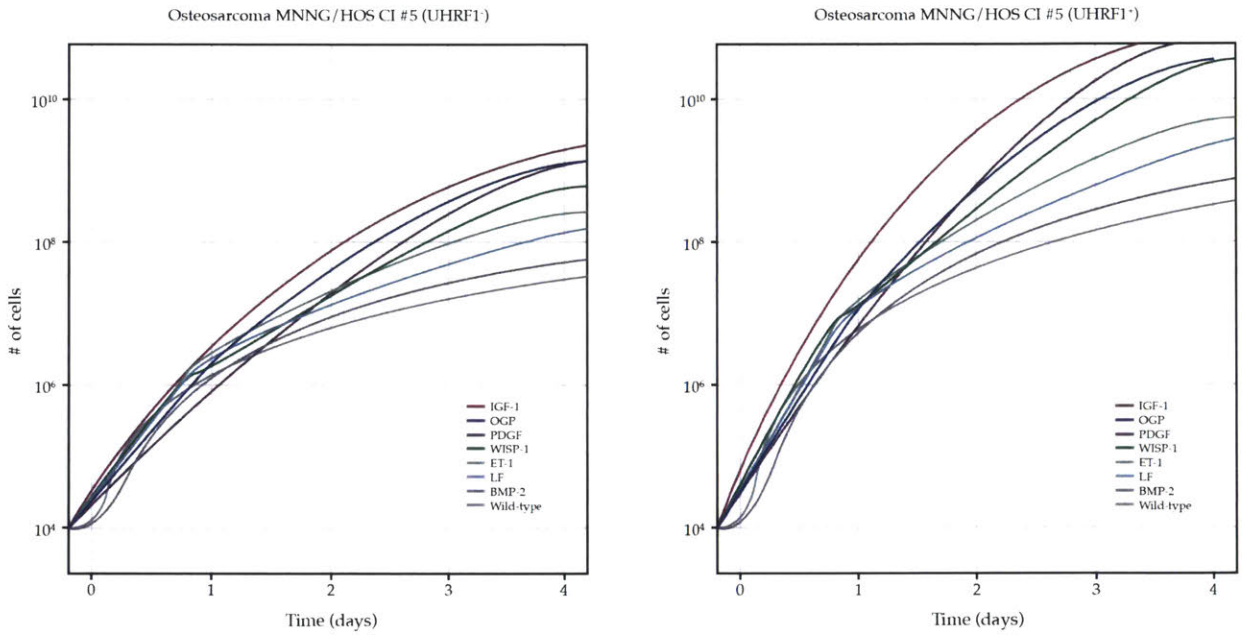

Figure 3.3 — Growth of osteosarcoma cell lines with and without *uhrf1* overexpression, in the presence of seven growth factors (BMP-2, LF, ET-1, WISP-1, PDGF, OGP, and IGF-1). The medium was changed every two days and all experiments were performed in triplicate.

Next, I tried the same experiment with Chondrosarcoma (uhrf1$^+$ and uhrf1$^-$) cells. Across all conditions, the population growth rate of chondrosarcoma cell lines was approximately 1/3 – 1/2 that of osteosarcomas. This means that the timing of any biofabrication process combining the two cell lines should be carefully considered.

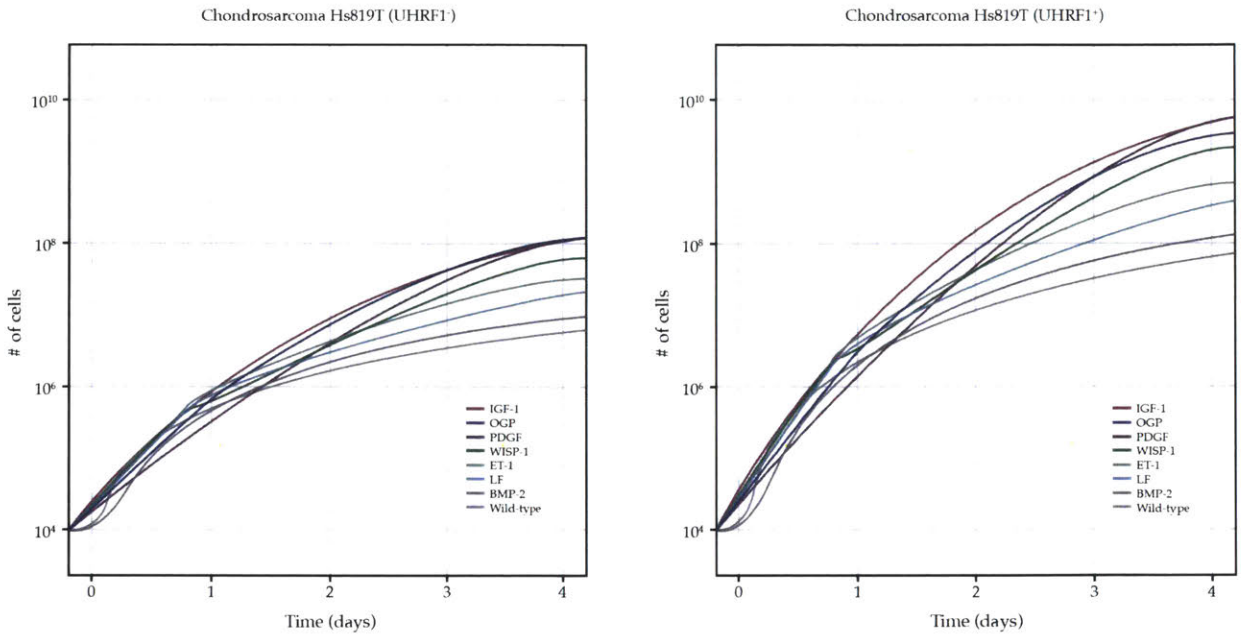

Figure 3.4 — Growth of chondrosarcoma cell lines with and without *uhrf1* overexpression, in the presence of seven growth factors (BMP-2, LF, ET-1, WISP-1, PDGF, OGP, and IGF-1). The medium was changed every two days and all experiments were performed in triplicate.

Finally, I grew the same number of osteosarcoma and chondrosarcoma cells with and without *uhrf1* overexpression, in the same volume of growth media and in the presence of one of seven growth factors, inside of a hypoxia incubator chamber (StemCell Technologies, Vancouver, CA), to induce a more aggressive phenotype. The atmospheric composition inside the chamber was 1% O_2, 5% CO_2, and 94% N_2,[60] which was confirmed using a single flow gas meter attached to the hypoxia incubator chamber (StemCell Technologies #27310, Vancouver, CA). In combination, UHRF1-overexpressing osteosarcoma cells in the presence of hypoxic conditions and exposed to insulin-like growth factor-1 (IGF-1) approximately doubled their population every 1.5 hours.

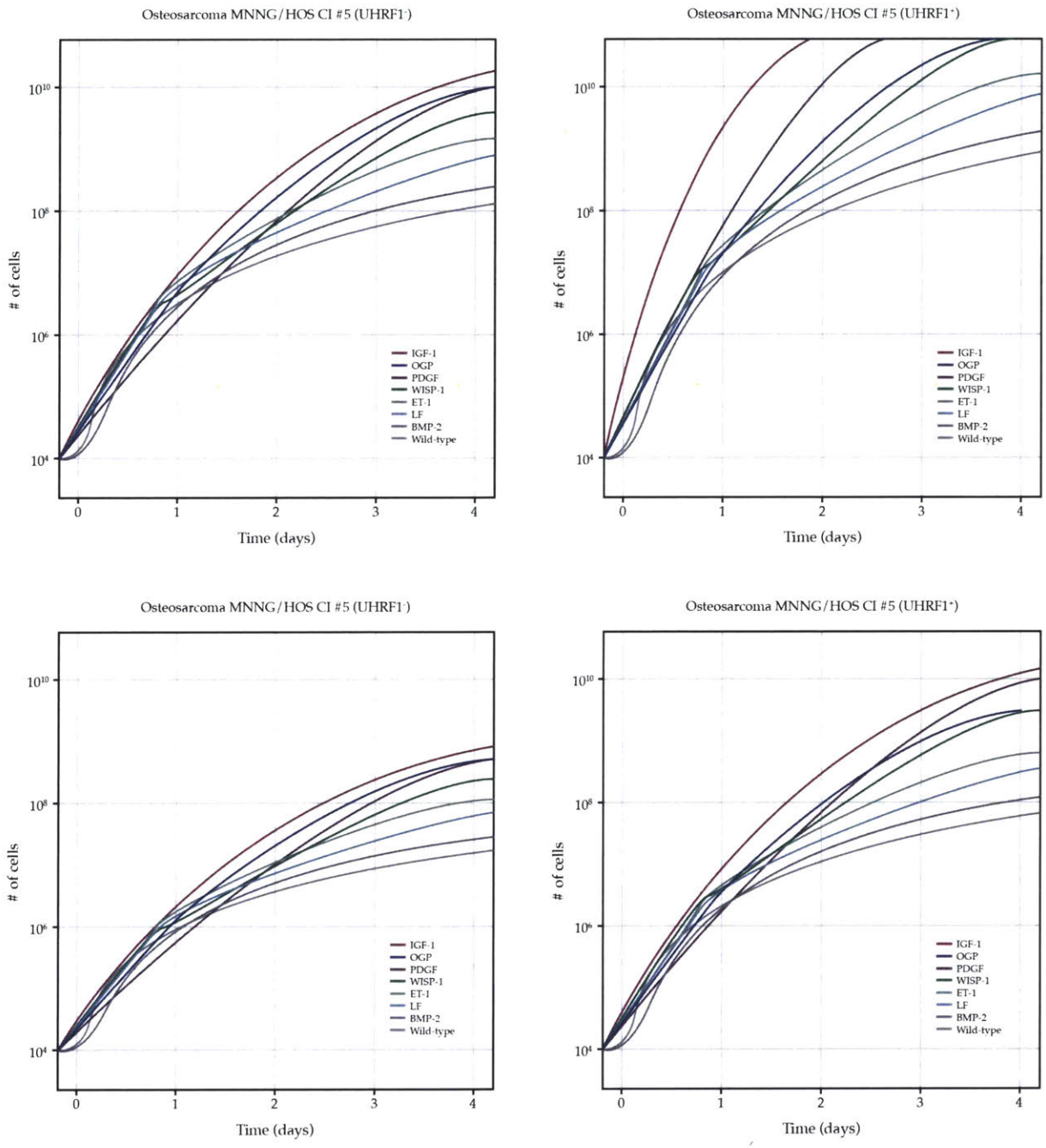

Figure 3.5 — Growth of osteosarcoma and chondrosarcoma cell lines (uhrf1$^+$ or uhrf1$^-$) in hypoxic conditions (1% O_2, 5% CO_2, and 94% N_2), in the presence of seven growth factors (BMP-2, LF, ET-1, WISP-1, PDGF, OGP, and IGF-1). The medium was changed every two days and all experiments were performed in triplicate.

It is important to note that these experiments should also be performed with *uhrf1* and *s100a10*-knockouts, different concentrations and combinations of growth factors, varying atmospheric conditions, a range of pressure on the cells (since bone growth occurs with weight on the cells), longer incubation periods, and in co-culture conditions. The growth rates should also be compared to those in three-dimensional culture, since mammalian cells behave much differently in two-dimensional and three-dimensional environments.[61] Moreover, genome sequencing and protein expression — especially UHRF1, S100A10, HIF-1α, MMP-9, and p53[62] — as well as cartilage and bone formation should be compared across cell lines and conditions to look for varying levels of each, especially between triplicate experiments. In this vein, it would also be good to do experiments with cells that have combinations of gene knockouts preventing the production of these proteins. These experiments will be performed in the near-future.

Three-dimensional Environment: With this information, I designed a simple hydrogel that would provide the cells with the building blocks they needed to make bone and cartilage, as well as mechanical and spatial signals that mediated density, metastasis, and tissue formation. Briefly, Noble agar (VWR, Radnor, PA) was mixed at concentrations of 1.5-2.5% (w/v) in distilled water. Octacalcium phosphate (Sigma-Aldrich, St. Louis, MO) was added at concentrations of 0.1-0.4% (w/v), so the osteosarcoma cells could form hydroxyapatite crystals.[63] The mixture was then mixed at 40°C for 20 minutes, then autoclaved for 20 minutes. Subsequently, the solution was stirred again on a magnetic stirrer until it cooled to 55°C, at which point an anti-mycotic was added.

After the mixture cooled to 40°C, it was parsed into eight T25 tissue culture flasks and pipetted with one of seven growth factors (10ng/ml). Five milliliters of osteosarcoma cells were pipetted into the center of the solution, after it had cooled to 37°C. The cooled gel remained solid at 37°C and did not deform significantly in an incubator. The flasks were incubated in a hypoxia incubator for ten days. Cell growth and bone formation were evaluated visually, with a microscope, and using Alizarin red staining, respectively.

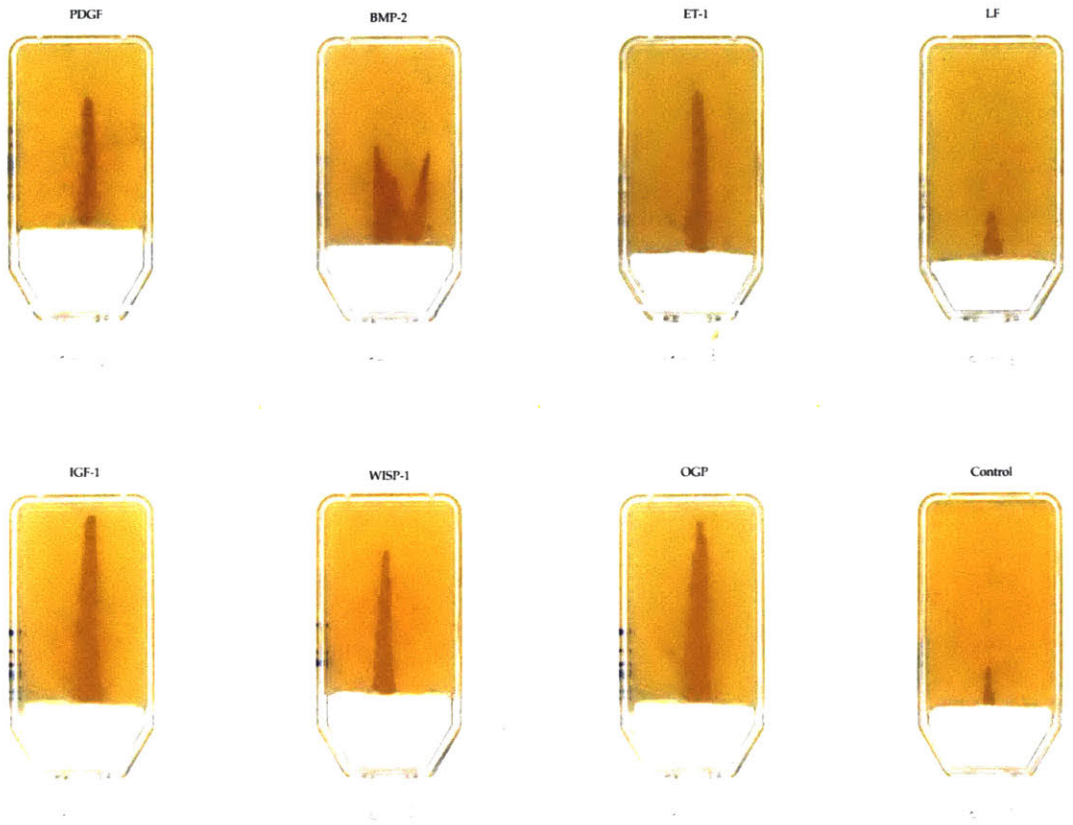

Figure 3.6 — Three-dimensional growth experiments using osteosarcoma cells in the presence of one of seven growth factors, in hypoxic conditions, over ten days. Alizarin red staining confirmed the presence of mineralized bone. Photo: Joe Kennedy.

Noble agar was chosen because this gel is used in some electrophoretic and immunodiffusion applications, and can therefore be used to sort proteins based on charge, size, and affinity. Doing so can enable spatial segregation of bioactive peptides and antibodies to guide the growth of heterogeneous cell populations. In addition, agar provides tunable and sufficient stiffness and porosity to enable bone and cartilage formation, as well as cell migration. The stiffness of gels made using different concentrations of agar and octacalcium phosphate will be measured using AFM operating in QI mode, which can also be utilized to determine cell attachment. Although I have not yet gotten to these research tracks, I will begin the experiments soon.

3.6 Biofabrication

The ultimate goal of the aforementioned experiments was to build up a tool palette with which to direct the growth and material production of two engineered bone cancer cell lines. In particular, modulating cell density, material distribution between hard bone and soft cartilage, micro-scale tissue geometry, and the porosity of the cellular solid can enable significant tunability and functional gradation of properties such as elasticity, strength-to-weight ratio, surface area maximization, and resilience, among others.

To do so, it will again be necessary to utilize fabrication information modeling[21] to integrate different design parameters across various time and length scales to gain any control over the multitude of parameters that elicit very different behaviors in cancer cells. A general design framework and workflow for a conditional adversarial network (CAN) that addresses the inverse problem as it pertains to heterogeneous cancer cell growth[64] and material production is presented below.

Briefly, working backward from the desired two-dimensional horizontal slice of a 3D computer-aided design (CAD) model, bioactive peptides, different cell densities, varying material stiffness and porosity, graded oxygen tension, specific cell attachment sites, and molecular sensors can be distributed to materialize the desired shape and hierarchical properties in a bioprinting process.

This information can be derived from local and global performance requirements of the structure itself such as thermal conductivity, strength-to-weight ratio, functional gradation, and responsiveness to changing climatic conditions, as well as ecological responsibilities such as self-healing to minimize resource usage to heal cracks or put up a new building, on-site conversion of waste to energy using reservoirs of engineered cells embedded in the building material, air filtration, and degradation back into the resource cycles the cells came from.

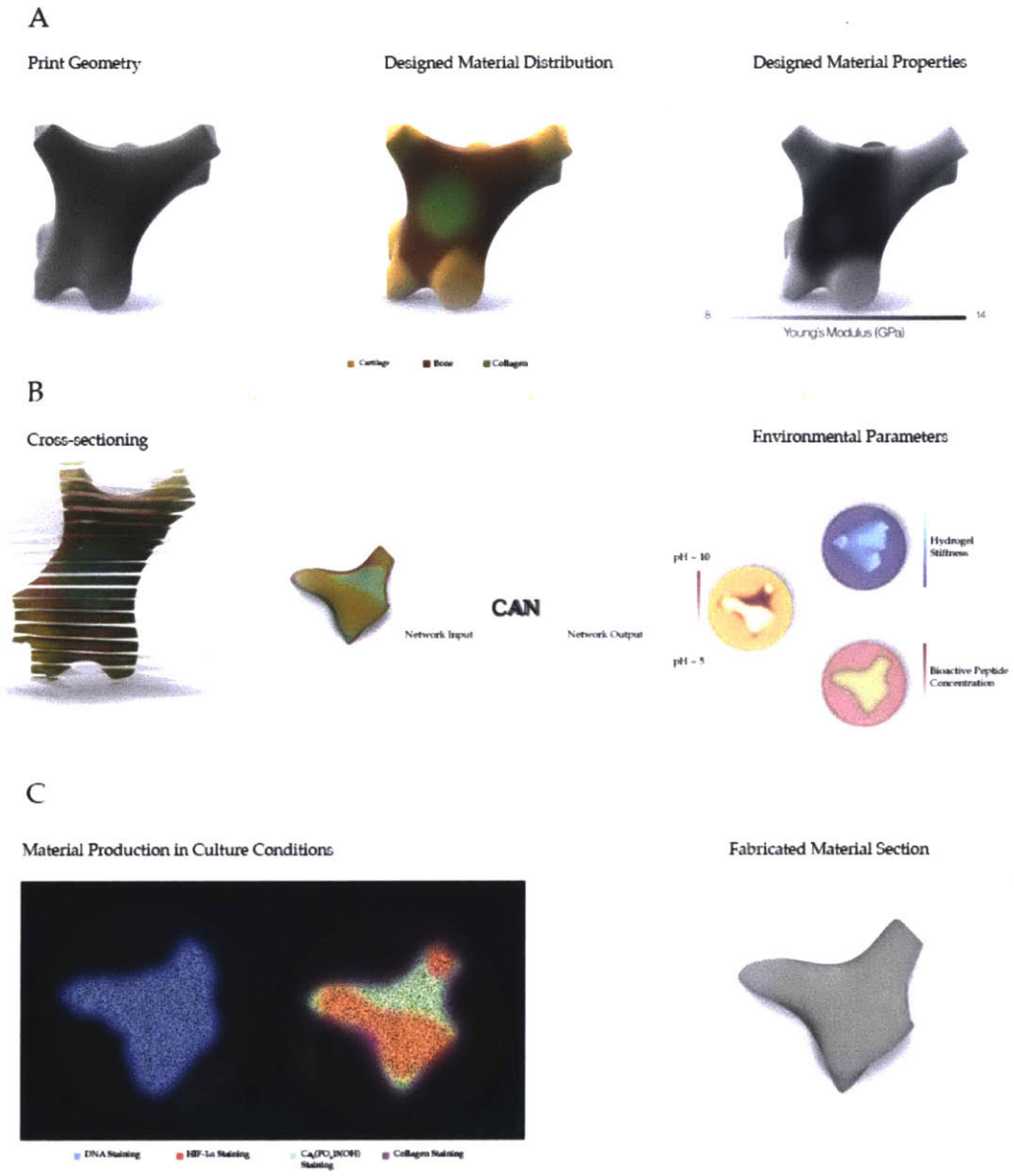

Figure 3.7 — An integrated workflow for the design, fabrication, and modification of hydrogel-based biofabrication environments. (**a**) Visual metadata encodes the desired material at each point in a voxel-based CAD model. (**b**) The model is cross-sectioned and the visual data is input into a trained CAN to identify genetic and environmental parameters required to induce cellular density and the micro-scale geometry of material production. (**c**) Multi-material sections are produced via cultured tumor cells.

Large-scale Experiments: To prove that the genetic and environmental manipulations I had tested in previous experiments could be implemented to grow bone structures at an architecturally meaningful scale, I pipetted 10 ml of osteosarcoma cells (10^8 cells/10 μl of media) that were overexpressing *uhrf1* and *s100a10* into an airtight Erlenmeyer flask containing 800 ml of the agar/octacalcium phosphate hydrogel (2.5% agar, 0.4% octacalcium phosphate, 0.5% anti-mycotic, 1% neomycin), while it was still liquid at 40°C. Cells were grown in hypoxic conditions (1% O_2, 5% CO_2, and 94% N_2,[60]), in the presence of all seven growth factors used in the initial proliferation experiments mentioned in section 3.5. New cells were carefully pipetted every two days within a circular boundary to create a three-dimensional column.

The growth medium was changed every two days, and the hypoxic chamber was monitored and filled daily. After three weeks of growth, a sufficiently large bone structure had been created, weighing only 275 grams. This is less than a male knee cap of comparable size.[65] While I have not yet tested the compressive or tensile strength of this structure — mostly because it is very hard to find a materials science laboratory willing to let me put a giant bone tumor onto its load cell — I will soon begin experiments in which I grow bone and cartilage structures into ASTM-standard molds to test on tensile, compressive, and micro-hardness testers.

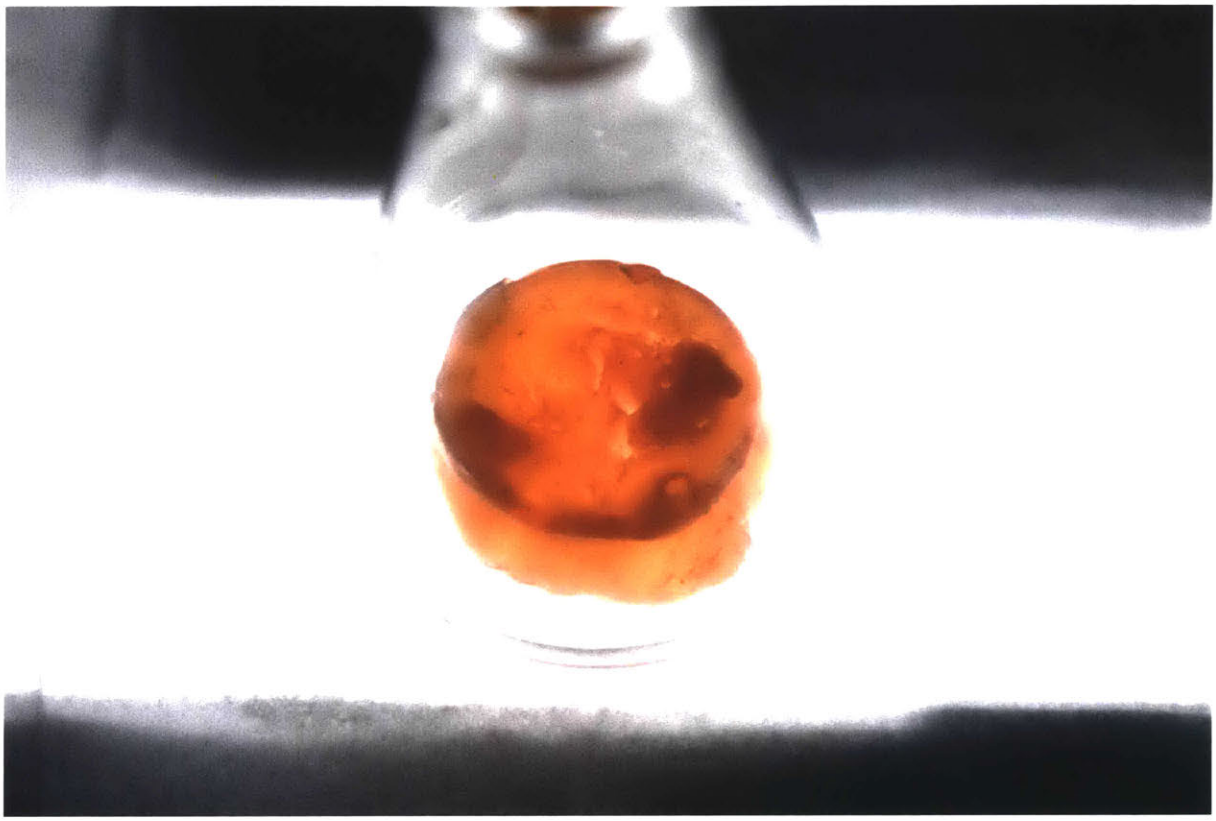

Figure 3.8 — Large-scale culture experiment using osteosarcoma cells grown in the presence of seven growth factors, in hypoxic conditions. Alizarin red staining was used to determine the presence of mineralized bone. Photo: Joe Kennedy.

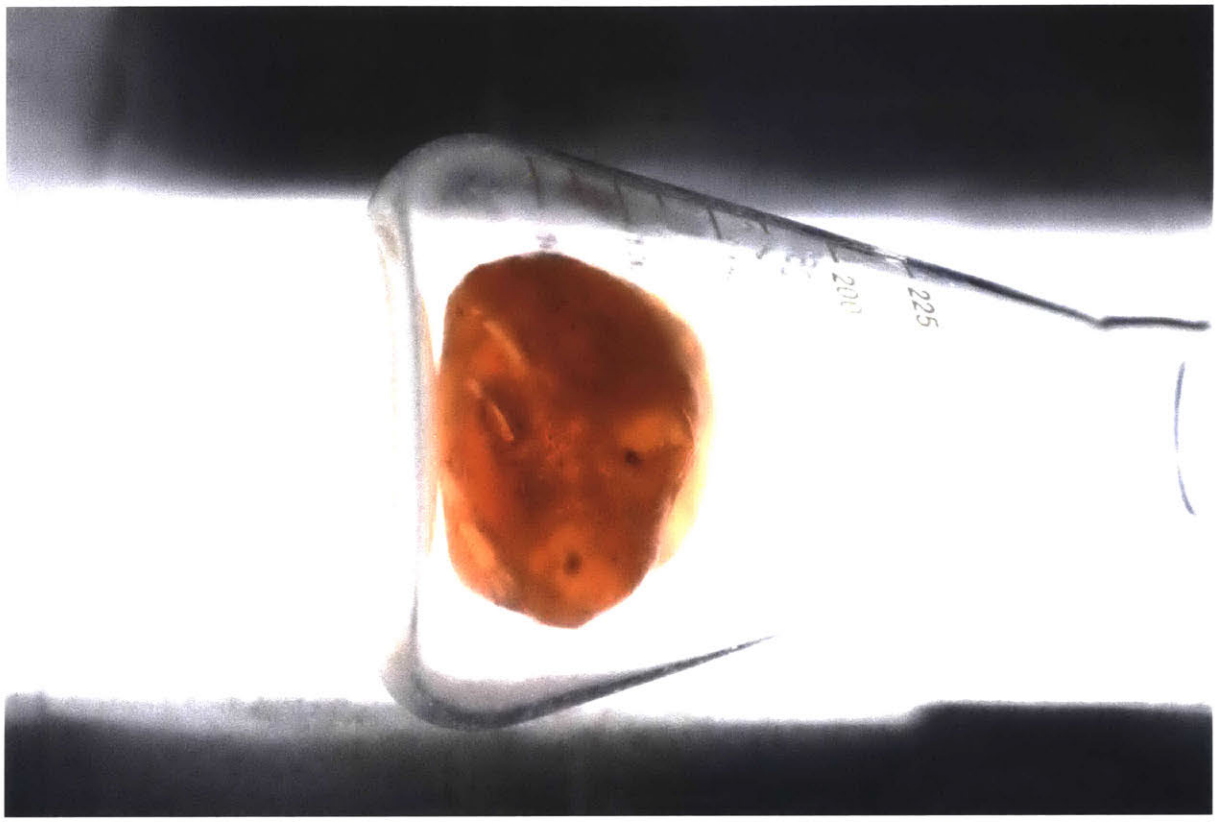

Figure 3.9 — Large-scale culture experiment using osteosarcoma cells grown in the presence of seven growth factors, in hypoxic conditions. View from underneath. Alizarin red staining was used to determine the presence of mineralized bone. Photo: Joe Kennedy

3.7 Conclusions

While I have only completed the first steps in growing building materials and entire structures using bone cancer cell lines, I believe that I have made exciting discoveries and good progress toward this goal. Specifically, I have figured out how to grow the biggest tumors within the shortest possible period of time, and am now excited to explore how to direct these cells to grow into beautiful, ecofunctional structures that demonstrate the utility of ecosystemic, rather than infrastructural, design.

In particular, utilizing the extracellular matrix to immobilize bioactive peptides will help refine the directionality of growth signaling. To do so, utilizing CAR-T cells to produce nanobodies with growth factor fusion proteins is a promising method of precisely manipulating the extracellular matrix of cells. Doing so can help direct the density, directionality, geometry, and distribution of tissue formation in heterogeneous cell populations. In this vein, selectively coating functionally graded hydrogels using different cell-attachment sites may enable tuning of micro-scale geometry as well as the creation of joints made of cartilage to deflect stresses and enable motion in response to changing environmental conditions. Conversely, more specific properties can be encoded into DNA-based hydrogels, which may offer the best control over such parameters. The problem here is scalability.

Moreover, using photopolymer-based hydrogels can enable selective stiffening to control cell density, cargo capture and release, and tissue growth direction in real time. I would also like to embed molecular sensors to monitor and alter environmental conditions in real time, thereby expanding the design space of biofabrication. These include pH — a key modulator of cancer cell growth — charge gradients, temperature, pressure, the presence of specific proteins, and many other factors that provide important signals to cells. This is also important because in biofabrication, printed cells continue to change over time, which can be considered an unwelcome complexity or an opportunity for added functionality.

Once sufficient control over cellular growth and tissue formation has been achieved, it will be necessary to analyze the resulting structures in terms of material, mechanical, and functional

properties, in order to optimize specific subsets of each for particular performative and ecosystemic functions. Doing so will require integrating tools and techniques across multiple length and time scales into a design workflow that considers many parameters and functions simultaneously, in order to generate optimal forms and material distributions.

I have made sure to include experiments that are either in progress or will be done in the near future to indicate that sufficient probing into biological phenomena will be performed. More importantly, though, I want to communicate the exciting directions this research can be taken based on early experimental success.

The ultimate goal of this research will be to realize an entire architectural structure that is beautiful and kills surface-adherent pathogens, filters the air and photosynthesizes, converts waste into energy, coordinates thought processes, autonomously evolves new capabilities, and even asexually reproduces. While this may seem like science fiction, it is often in science fiction that our most ambitious goals are made known to the world. These have included computers, self-driving and flying cars, robots, artificial intelligence, and transhumanism, among other imagined solutions to complex global problems that are now within reach.

I hope that the people who read this thesis consider this a useful theoretical framework that causes them to reconsider how we build our habitats. With the knowledge, opportunities, and permissionless ambition I have gained at MIT, I will work toward proving the utility of and actually materializing ecofunctional infrastructure that participates in the construction and maintenance of our planet. Thus, I would like to thank anyone who has taken the time to read this thesis through. I hope you have gotten something useful out of it.

References

1. Oxman, N. Towards a Material Ecology. World Econ. Forum (2016).
2. Van Zak, J. et al. Parametric Chemistry: Reverse-engineering Biomaterial Composite Structures for Robotic Manufacturing of Bio-Cement Structures across Scales. in Towards a Robotic Architecture (Edited by Andrew Wit and Mahesh Daas).
3. H.P.S, A. K. et al. A review on chitosan-cellulose blends and nanocellulose reinforced chitosan biocomposites: Properties and their applications. Carbohydr. Polym. **150**, 216–226 (2016).
4. Lankalapalli, S. & Kolapalli, V. R. M. Polyelectrolyte complex: a review of their applicability in drug delivery technology. Indian J. Pharm. Sci. **71**, 481–487 (2009).
5. Liu, H. & et al. Effect of electrostatic interactions on the structure and dynamics of a model polyelectrolyte. I. Diffusion. J. Chem. Phys. **109**, 7556–7666 (1998).
6. Dakhara, S. & Anajwala, C. Polyelectrolyte complex: A pharmaceutical review. Syst. Rev. Pharm. **1**, 121 (2010).
7. Deeksha & Rishabha Malviya and Pramod Kr. Sharma. Poly-Electrolyte Complex: A Novel System for Biomedical Applications and Recent Patents. Recent Pat. Nanotechnol. **8**, 129–141 (2014).
8. Kalpana, R., Park, K. & Kamath. Biodegradable hydrogels in drug delivery. Adv. Drug Deliv. Rev. **11**, 59–84 (1993).
9. Ponnamma, D. et al. Advanced Structured Materials. in **11**, (2013).
10. Kulkarni, A. D. et al. Polyelectrolyte complexes: mechanisms, critical experimental aspects, and applications. Artif. Cells Nanomedicine Biotechnol. **44**, 1615–1625 (2016).

11. Mogas-Soldevila, L., Duro-Royo, J. & Oxman, N. Water-Based Robotic Fabrication: Large-Scale Additive Manufacturing of Functionally Graded Hydrogel Composites via Multichamber Extrusion. 3D Print. Addit. Manuf. **1**, 141–151 (2014).

12. Tu, H. et al. Highly cost-effective and high-strength hydrogels as dye adsorbents from natural polymers: chitosan and cellulose. Polym Chem **8**, 2913–2921 (2017).

13. Tai, Y. J. Towards material-informed tectonics. (Massachusetts Institute of Technology, 2019).

14. Van Zak, J. et al. Methods and Apparatus for Parametric Fabrication.

15. Meka, V. et al. A comprehensive review on polyelectrolyte complexes. **22**, (2017).

16. Whyman, G., Bormashenko, E. & Stein, T. The rigorous derivation of Young, Cassie–Baxter and Wenzel equations and the analysis of the contact angle hysteresis phenomenon. **450**, (2008).

17. J. Jasper, W. & Anand, N. A generalized variational approach for predicting contact angles of sessile nano-droplets on both flat and curved surfaces. **281**, (2019).

18. Wilhelm Barthlott, Matthias Mail, Bharat Bhushan & Kerstin Koch. Plant Surfaces: Structures and Functions for Biomimetic Innovations. Nano-Micro Lett. **9**, (2017).

19. Shafrin, E. G. & Zisman, W. A. Constitutive Relations in the Wetting of Low Energy Surfaces and the Theory of the Retraction Method of Preparing Monolayers. J. Phys. Chem. **64**, 519–524 (1960).

20. Ling, A. S. Design by decay, decay by design. (Massachusetts Institute of Technology, 2019).

21. Duro Royo, J. Towards Fabrication Information Modeling (FIM) : workflow and methods for multi-scale trans-disciplinary informed design. (2015).

22. Winner, W. & Atkinson, C. Annual Absorption of Gaseous Air Pollutants by Mosses and Vascular Plants in Diverse Habitats. (1987). doi:10.1007/978-3-642-70874-9_31

23. Van der Velde, M., During, H. J., Van de Zande, L. & Bijlsma, R. The reproductive biology of Polytrichum formosum: clonal structure and paternity revealed by microsatellites. Mol. Ecol. **10**, 2423–2434 (2001).

24. Tai, Y. J., Bader, C. & Ling, A. S. Designing Decay: Parametric Material Distribution for Controlled Dissociation of Water-based Biopolymer Composites. in Proceedings of the IASS Symposium 2018 (Edited by Caitlin T. Mueller and Sigrid Adriaenssens, 2018).

25. Koyama, M. et al. Bone-like crack resistance in hierarchical metastable nanolaminate steels. Science **355**, 1055–1057 (2017).

26. North, L. et al. Interrelated chemical-microstructural-nanomechanical variations in the structural units of the cuttlebone of Sepia officinalis. **5**, (2017).

27. Gibson, L. J. & Ashby, M. F. Cellular Solids: Structure and Properties. (Cambridge University Press, 1997). doi:10.1017/CBO9781139878326

28. Ben-David, U. et al. Genetic and transcriptional evolution alters cancer cell line drug response. Nature **560**, 325–330 (2018).

29. Dietrich, M. et al. Guiding 3D cell migration in deformed synthetic hydrogel microstructures. Soft Matter **14**, 2816–2826 (2018).

30. Zhang, M. & Zhang, X. Association of MMP-2 expression and prognosis in osteosarcoma patients. Int. J. Clin. Exp. Pathol. **8**, 14965–14970 (2015).

31. Baek, N., Seo, O. W., Lee, J., Hulme, J. & An, S. S. A. Real-time monitoring of cisplatin cytotoxicity on three-dimensional spheroid tumor cells. Drug Des. Devel. Ther. **10**, 2155–2165 (2016).

32. Sohn, L. L. Fields, Forces, and Flows in Biological Systems edited by Alan J. Grodzinsky and Eliot H. Frank. Q. Rev. Biol. **87**, 159–159 (2012).

33. Charoen, K. M., Fallica, B., Colson, Y. L., Zaman, M. H. & Grinstaff, M. W. Embedded multicellular spheroids as a biomimetic 3D cancer model for evaluating drug and drug-device combinations. Biomaterials **35**, 2264–2271 (2014).

34. Rocca, M., Fragasso, A., Liu, W., Heinrich, M. A. & Zhang, Y. S. Embedded Multimaterial Extrusion Bioprinting. SLAS Technol. **23**, 154–163 (2018).

35. Li, M., Feng, C., Gu, X., He, Q. & Wei, F. Effect of cryopreservation on proliferation and differentiation of periodontal ligament stem cell sheets. Stem Cell Res. Ther. **8**, 77–77 (2017).

36. Forsythe, J. G. et al. Surveying the sequence diversity of model prebiotic peptides by mass spectrometry. Proc. Natl. Acad. Sci. U. S. A. **114**, E7652–E7659 (2017).

37. Kierdorf, U. & Kierdorf, H. Deer Antlers – A Model of Mammalian Appendage Regeneration: An Extensive Review. Gerontology **57**, 53–65 (2011).

38. Ker, D. F. E. et al. Identifying deer antler uhrf1 proliferation and s100a10 mineralization genes using comparative RNA-seq. Stem Cell Res. Ther. **9**, 292–292 (2018).

39. Beck, A. et al. Overexpression of UHRF1 promotes silencing of tumor suppressor genes and predicts outcome in hepatoblastoma. Clin. Epigenetics **10**, 27–27 (2018).

40. Noye, T. M., Lokman, N. A., Oehler, M. K. & Ricciardelli, C. S100A10 and Cancer Hallmarks: Structure, Functions, and its Emerging Role in Ovarian Cancer. Int. J. Mol. Sci. **19**, 4122 (2018).

41. Aldaye, F. A., Senapedis, W. T., Silver, P. A. & Way, J. C. A structurally tunable DNA-based extracellular matrix. J. Am. Chem. Soc. **132**, 14727–14729 (2010).

42. Park, N., Um, S. H., Funabashi, H., Xu, J. & Luo, D. A cell-free protein-producing gel. Nat. Mater. **8**, 432 (2009).

43. Park, N. et al. High-yield cell-free protein production from P-gel. Nat. Protoc. **4**, 1759 (2009).

44. Forget, A. et al. Mechanically Tunable Bioink for 3D Bioprinting of Human Cells. Adv. Healthc. Mater. **6**, 1700255 (2017).

45. Sen, K. S., Duarte Campos, D. F., Köpf, M., Blaeser, A. & Fischer, H. The Effect of Addition of Calcium Phosphate Particles to Hydrogel-Based Composite Materials on Stiffness and Differentiation of Mesenchymal Stromal Cells toward Osteogenesis. Adv. Healthc. Mater. **7**, 1800343 (2018).

46. Park, K. M. & Gerecht, S. Hypoxia-inducible hydrogels. Nat. Commun. **5**, 4075 (2014).

47. Park, K. M., Blatchley, M. R. & Gerecht, S. The design of dextran-based hypoxia-inducible hydrogels via in situ oxygen-consuming reaction. Macromol. Rapid Commun. **35**, 1968–1975 (2014).

48. Cheng, H. et al. Mussel-Inspired Multifunctional Hydrogel Coating for Prevention of Infections and Enhanced Osteogenesis. ACS Appl. Mater. Interfaces **9**, 11428–11439 (2017).

49. Wu, C., Bull, B., Christensen, K. & McNeill, J. Ratiometric single-nanoparticle oxygen sensors for biological imaging. Angew. Chem. Int. Ed Engl. **48**, 2741–2745 (2009).

50. Du, S. et al. Design and validation of a new ratiometric intracellular pH imaging probe using lanthanide-doped upconverting nanoparticles. Dalton Trans. **46**, 13957–13965 (2017).

51. Matsubara, T., Diresta, G. R., Kakunaga, S., Li, D. & Healey, J. H. Additive Influence of Extracellular pH, Oxygen Tension, and Pressure on Invasiveness and Survival of Human Osteosarcoma Cells. Front. Oncol. **3**, 199–199 (2013).

52. Uchiyama, S. et al. A cationic fluorescent polymeric thermometer for the ratiometric sensing of intracellular temperature. Analyst **140**, 4498–4506 (2015).

53. Rigueur, D. & Lyons, K. M. Whole-mount skeletal staining. Methods Mol. Biol. Clifton NJ **1130**, 113–121 (2014).

54. Zhu, H., Tang, J., Tang, M. & Cai, H. Upregulation of SOX9 in osteosarcoma and its association with tumor progression and patients' prognosis. Diagn. Pathol. **8**, 183–183 (2013).

55. Gonzalez-Campora, R., Otal Salaverri, C., Gomez Pascual, A., Hevia Vazquez, A. & Galera Davidson, H. Mesenchymal chondrosarcoma of the retroperitoneum. Report of a case diagnosed by fine needle aspiration biopsy with immunohistochemical, electron microscopic demonstration of S-100 protein in undifferentiated cells. **39**, (1995).

56. Sidhu, H. & Capalash, N. UHRF1: The key regulator of epigenetics and molecular target for cancer therapeutics. Tumor Biol. **39**, 1010428317692205 (2017).

57. Tanaka, N., Nishikawaji, T. & Ogama, N. Abstract 1109: S100A10 contributes to cancer stemness, invasion and metastasis of head and neck cancer cells. Cancer Res. **78**, 1109 (2018).

58. Lin, T.-C. et al. Leptin signaling axis specifically associates with clinical prognosis and is multifunctional in regulating cancer progression. Oncotarget **9**, 17210–17219 (2018).

59. Pigossi, S. C., Medeiros, M. C., Saska, S., Cirelli, J. A. & Scarel-Caminaga, R. M. Role of Osteogenic Growth Peptide (OGP) and OGP(10-14) in Bone Regeneration: A Review. Int. J. Mol. Sci. **17**, 1885 (2016).

60. Wang, G. L., Jiang, B. H., Rue, E. A. & Semenza, G. L. Hypoxia-inducible factor 1 is a basic-helix-loop-helix-PAS heterodimer regulated by cellular O2 tension. Proc. Natl. Acad. Sci. U. S. A. **92**, 5510–5514 (1995).

61. Damayanti, N. P. et al. Differentiation of cancer cells in two-dimensional and three-dimensional breast cancer models by Raman spectroscopy. J. Biomed. Opt. **18**, 117008–117008 (2013).

62. Cooper, G. M. Oncogenes. (Jones and Bartlett Publishers, 1995).

63. Suzuki, O. Octacalcium phosphate (OCP)-based bone substitute materials. **49**, (2013).

64. Gatenby, R. A., Maini, P. K. & Gawlinski, E. T. Analysis of tumor as an inverse problem provides a novel theoretical framework for understanding tumor biology and therapy. Appl. Math. Lett. **15**, 339–345 (2002).

65. Lee, G.-C., Cushner, F., Y Cannella, L. & Scott, W. The effect of total knee arthroplasty on body weight. **28**, (2005).